Title	昆虫病原性糸状菌Lecanicillium sp.が生産する抗真菌リポペプチド化合物verlamelinの生合成に関する研究
Author(s)	石堂, 圭一
Citation	大阪大学, 2014, 博士論文
Version Type	VoR
URL	https://doi.org/10.18910/52171
rights	
Note	

博士学位論文

昆虫病原性糸状菌 *Lecanicillium* sp.が生産する抗真菌リポペプチド化合物 verlamelin の生合成に関する研究

石堂　圭一

平成２６年　８月

大阪大学大学院工学研究科

Contents

Chapter 1

General introduction

1.1 Filamentous fungi as a source of bioactive compounds

1.1.1 Natural products

Despite diverse organisms present in nature, the common material (such as sugars, amino acids or fats) are utilized to construct, maintain or reproduce the cells. These compounds are produced via common pathway, and referred to as primary metabolites. On the contrary, there present the compounds which are synthesized using primary metabolites as constructing material and have limited distribution. These compounds are normally not essential for living cells and referred to as secondary metabolites.

It has been widely accepted that one of the important physiological roles of secondary metabolites is their specific biological interaction between the producing organisms and other organisms; competitors, invaders, predators or host organisms. The secondary metabolites produced for such purposes are usually highly active, which might be because they are created to confer advantages on the producer under severe natural competitions. Therefore, natural products produced as secondary metabolisms are regarded as molecules which have high potential to be developed as important chemicals for pharmaceutical industry and agroindustry.

Among over 500 thousands of natural products which have been known so far, about 1,200-1,300 (0.3%) are developed as medicine (Bérdy 2012). On the other hand, the

number of medicines developed based on synthetic chemical compounds was about 2,000-2,500. Thus, natural products are in tough competition with compounds with synthetic and combinatorial chemistries. However, regarding the ‘‘success rate’’, natural products are recognized as much more excellent source of drug seeds. Since the total number of chemically synthesized compounds is 8-10 millions, the ‘‘success rate’’ for finding drug seed is about 0.03%, which is more than 10 times lower than that of natural products (0.3%).

1.1.2 Microbial bioactive compounds

The largest population in natural products is plant-derived compounds (about 70%) (Bérdy 2012). However, regarding the bioactivity, more than half of compounds which show bioactivity are derived from microbes. Until the end of last century, majority of known microbial bioactive compounds were exclusively derived from actinobacteria, especially from *Streptomyces* sp.. Large numbers of *Streptomyces*-derived compounds were developed as important chemicals, as exemplified by clinically important antibiotics such as streptomycin, rifamycin, erythromycin and tetracycline. Meanwhile the population of fungal secondary metabolites in all microbial metabolites has expanded from the beginning of 1990th (Bérdy 2005). Today, fungal metabolites represent the largest population in microbial metabolites (45% of total microbial metabolites), which are from basidiomycetes (mushrooms; 11%) and microscopic

eukaryotic organisms (33%), such as filamentous fungi including *Penicillium*, *Aspergillus* and *Trichoderma* and hundreds of other species.

1.1.3 Fungal bioactive compounds

Filamentous fungi have been recognized as producers of bioactive compounds from the beginning of the study on bioactive compounds. One of the most famous antibiotics produced by filamentous fungi is ‘penicillin’, the name of which was given to an antibacterial activity of mold juice from *Penicillium notatum* in 1929 by Alexander Fleming (1929). The isolation of penicillin by Florey and Chain and its usefulness against bacterial pathogens inspired researchers all over the world to seek bioactive compounds, leading to the discovery of important bioactive compounds for clinical or agrochemical use (Fig. 1.1).

Regarding the compounds developed as medicine, there present remarkable bioactive compounds from filamentous fungi. One of the most notable medicine is immunosuppressive drug cyclosporine which is produced by *Tolypocladium inflatum* (Fig. 1.1). Cyclosporine has cyclic peptide structure and exhibits a narrow range of antifungal activity, but high levels of immunosuppressive and anti-inflammatory activities (Dewick 2009). It has revolutionized organ transplant surgery, substantially increasing survival rates in transplant patients.

Another important medicine from filamentous fungi is lovastatin produced by

Monascus ruber (Fig. 1.1). Lovastatin was shown to be reversible competitive inhibitor of HMG-CoA reductase, dramatically lowering sterol biosynthesis in mammalian cell cultures and animals, and reducing total and low-density lipoprotein (LDL) cholesterol levels (Dewick 2009).

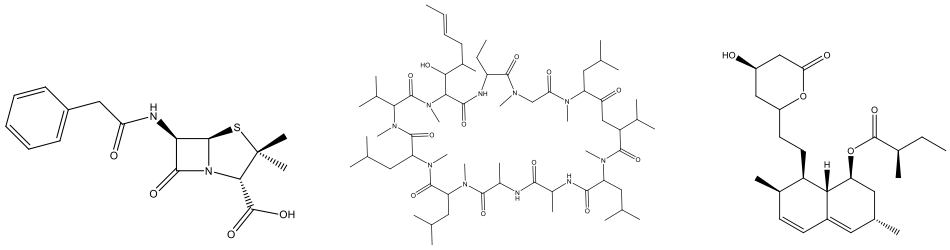

penicillin G cyclosporine lovastatin

Fig. 1.1. Representative of bioactive compounds produced by filamentous fungi.

1.2 Cyclic lipopeptide

1.2.1 General information

Lipopeptide compounds consist one grope of secondary metabolites when classified based on structure or constructing materials. Lipopeptides are low molecular weight compounds which have linear or cyclic oligo-peptide substructure linked with lipid or other lipophilic molecule. Since some of them have anti-microbial/viral activity, properties as surfactant, and especially those with cyclic peptide structure are peptidase resistant, they are utilized in cosmetic, food and pharmaceutical industry.

Surfactin (Fig. 1.2), anti-microbial cyclic lipopeptide produced by *Bacillus subtillis* has received highest attention with its multiple use in the industry because of its

exceptionally high surface property (Mandal et al. 2013). Moreover, it has low toxicity to human cells and minor irritation to human skin. Therefore, in the cosmetic industry, derivatives of surfactin have been used for dermatological products and for cleansing cosmetics with highly washable capacities. In addition to these application in cosmetic industry, surfactin has been used as a food additive. In baking industry, surfactin has been used as emulsifier, to maintain stability, texture and volume of products, and also to help in the emulsification of fat tissue in order to control fat globule glomeration.

Because of the continuous emergency of multi-drug-resistance bacteria, novel anti-bacterials have been always demanded in pharmaceutical industry. Daptomycin (Fig. 1.2), anti-bacterial lipopeptide against Gram-positive bacteria was isolated from *Streptomyces roseosporum* and was approved in the USA in 2003 for the treatment of complicated skin and soft tissue infections. It exhibited anti-bacterial activities against 15 Gram-positive genera including 35 species and the minimal inhibitory concentration (MIC) was less than 1 μg/ml for most of the tested strain (Baltz et al. 2005). Importantly, daptomycin is active against methicillin-resistant *Staphylococcus aureus* (MRSA), vancomycin-resistant *Enterococci* (VRE) and penicillin-resistant *Staphylococcus pneumonia* (PRSP).

As for the lipopeptide produced by filamentous fungi, echinocandin-type anti-fungal lipopeptide would be notable. Echinocandin was isolated from *Aspergillus nidulans* during screening program for new antifugal agent (Fig. 1.2). Although echinocandin

shows anti-*Candida* activity, its strong hemolytic activity hampered the clinical use (Cacho et al. 2012). Chemical derivatization of echinocandin in the fatty acid side chain led to the development of anidulafungin (trade name; Eraxis, Pfizer), which has lower hemolytic activity than original compound while the antifungal activity was maintained.

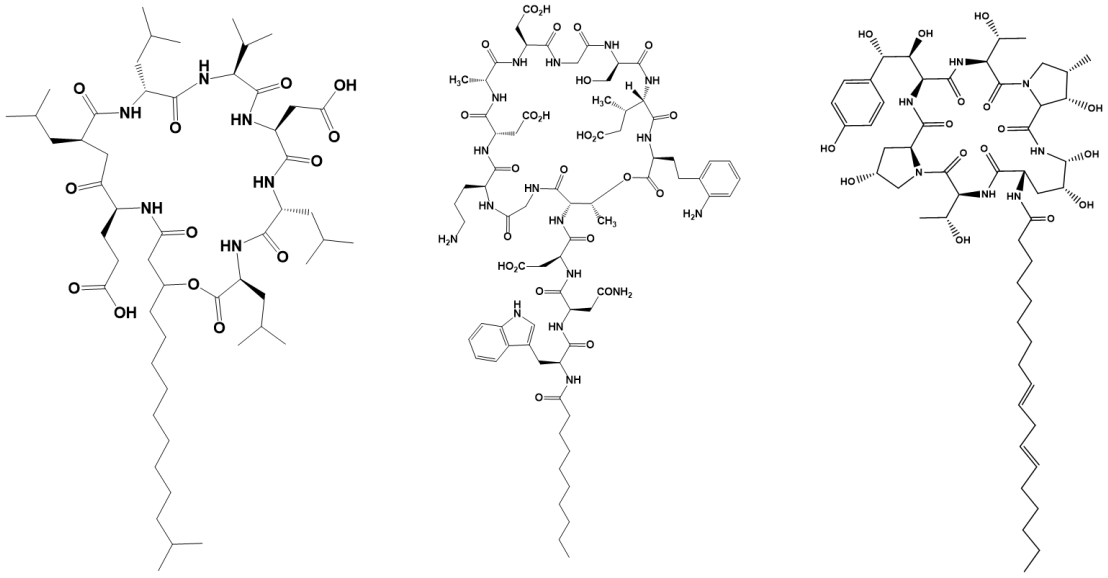

Fig. 1.2. Representative of cyclic lipopeptide compounds.

1.2.2 Mode of actions

The proposed primary mode of action of cyclic lipopeptide is pore formation in membrane, leading to an imbalanced transmembrane ion fluxes and cell death (Mandal et al. 2013). In the case of daptomycin, calcium binding with daptomycin cause a conformational change, which facilitate binding to membrane. Further conformational

change occurred by interacting with the negatively charged head group of phosphatidylglycerol, which lead to oligomerization and deeper membrane insertion of daptomycin, resulting in the formation of ion-conducting pore (Muraih et al. 2011). Although not so detailed studies as daptomycin have yet been conducted on surfactin and iturin, both of which are produced by *Bachillus subtillis*, several studies suggested that the mode of action of them are similar to daptomycin (Aranda et al. 2005; Ostroumova et al. 2010).

In addition, some research has indicated that cyclic lipopeptide shows antifungal activities via other mode of actions than pore formation in membrane. Fengycin (identical to plipastatin), antifungal cyclic lipopeptide produced by *Bachillus subtillis*, have 40-times less haemolytic activity than surfactin (Deleu et al. 2005), which suggested that the mode of action of this cyclic depsipeptide was not membrane permeabilizing. Enzyme inhibition assay indicated that plipastatin A1 has inhibitory activity against phospholipase A_2. Meanwhile, echinocandin type antifungal lipopeptides were shown to act by specific and non-competitive inhibition of enzyme 1,3-β-glucan synthase (Wiederhold et al. 2003). Since this polysacchalide is essential as cell wall components of fungi including *Aspergillus* or *Candida*, the inhibition of 1,3-β-glucan synthase lead to the cell death of these opportunistic pathogens.

Taking these facts together, hydrophobicity or amphiphilicity should be the most important physical properties of lipopeptide compounds, since they interact with

transmembrane protein or the enzyme working at a water/lipid interface (Douglas et al. 1994; Gelb et al. 1994), or membrane of microbial cells. Therefore, lipophilic substructure, which confer hydrophobicity on the peptide cores, might be commonly important for the bioactivity of lipopeptide compounds.

1.3 Biosynthesis of fungal secondary metabolites

Although fungal secondary metabolites have diverse structures and various biological aspects, such as pathogenic factors, food contaminants and industrially important chemicals, all the starting materials and components are from primary metabolites. Therefore, based on the component materials for the biosynthesis, fungal secondary metabolites can be mainly classified into polyketides, peptides and isoprenoids (Keller et al. 2005).

1.3.1 Polyketide biosynthesis

Polyketides are synthesized from acyl-CoA and malonyl-CoA, and share common materials with fatty acid biosynthesis. Polyketides are synthesized by multifunctional enzyme, polyketide synthase, which have similar domains to fatty acid synthase (Shimizu 2006$_a$). Ketosynthase (KS) domain mediates the decarboxylative condensation between acyl and malonyl groups which are transferred from acetyl and malonyl CoA by acyl transferase (AT) domain to give a β-ketothioester. Further reactions are

catalyzed by ketoreductase (KR) domain, enoylreductase (ER) domain, and dehydratase (DH) domain on the β-ketothioester group with acyl carrier protein (ACP) domain. The products were released from PKS by thioesterase (TE) domain or reductase (R) domain afterward. Fungal PKS has only a single set of these domains which are iteratively used, like fatty acid synthase, but unlike bacterial modular PKS.

Both polyketide synthase and fatty acid synthase elongate the primary chain by condensation of malonyl-CoA as the extender and reduce each β-carbon in similar manner. However, structural diversities of polyketide compounds are derived from the optional and partial reduction of β-carbons, while all β-carbons are fully reduced in the fatty acid biosynthesis (Fig. 1.3).

1.3.2 Isoprenoid biosynthesis

Isoprenoids are composed of linearly conjugated units that contain five carbons in the branched chain structure, called as isoprene. The initial step involves biosynthesis of the C_5 compounds, isopentenyl diphosphate (IPP) and its isomer, dimethylallyl diphosphate (DMAPP). Two independent isoprenoid pathway, the mevalonate pathway and the methylerythritol pathway, have been discovered. Fungal isoprenoids are synthesized via mevalonate pathway, where two molecules of acetyl-CoA are used as starting materials to synthesized IPP or DMAPP (Singkaravanit 2010_a). In the next step, the IPP is conjugated with DMAPP to form the linear C10 diphosphate precursor (geranyl

diphosphate) and longer polyprenyl diphosphate precursors. Then, these precursors are cyclized and/or rearranged in the linear molecules to form the primary isoprenoid carbon backbone. The skeletons are tailored or modified by tailoring enzymes into final compounds afterward. The representatives of fungal isoprenoids are shown in Fig. 1.3.

1.3.3 Non-ribosomal peptide biosynthesis

In microbial secondary metabolism, a number of peptide compounds of low molecular weight were known to be synthesized by non-ribosomal peptide synthetases (NRPSs) (Jirakkakul et al. 2008; Slightom et al. 2009; Wiest et al. 2002; Xu et al. 2008). NRPS is a multifunctional enzyme composed of modules, each of which contains catalytic domains in a row, corresponding to the order of amino acids in the structure of peptide compounds (Marahiel et al. 1997). Three essential domains, adenylation (A) domain, peptidyl carrier protein (PCP) domain and condensation (C) domain, are required to elongate peptide, which usually arrange in an order of C-A-PCP in a module. Amino acid substrates are delivered and covalently linked to phosphopantetheinyl groups on PCP domains as aminoacyl adenylates after activation by A domains. C domains sequentially form amide bonds by condensation of amino group to neighboring aminoacyl thioester with nucleophilic attack (Fig. 1.4). Products by NRPSs are structurally more diverse than those by ribosome, because NRPSs can utilize broader substrates and modify amioacyl thioesters by methylation, cyclization and/or

epimerization catalyzed by corresponding domains (Fig. 1.3).

Although a number of non-ribosomal peptide biosynthesis have been studied, only a few studies have been reported on detailed biosynthesis of lipopeptides which contain a long/middle-chain fatty acid moiety, such as emericellamide, apicidin or echinocandin (Cacho et al. 2012; Chiang et al. 2008; Jin et al. 2010). All identified biosynthetic gene clusters of fungal lipopeptides contain NRPS genes, the products of which represent the peptide moieties of lipopeptide. In contrast to the peptide moieties synthesized by NRPS, the knowledge about biosynthesis of the fatty acid moieties has not been accumulated because of less number of studies available. Therefore, considering the aspect of fatty acid moieties, fungal lipopeptide biosynthesis still remain to be investigated.

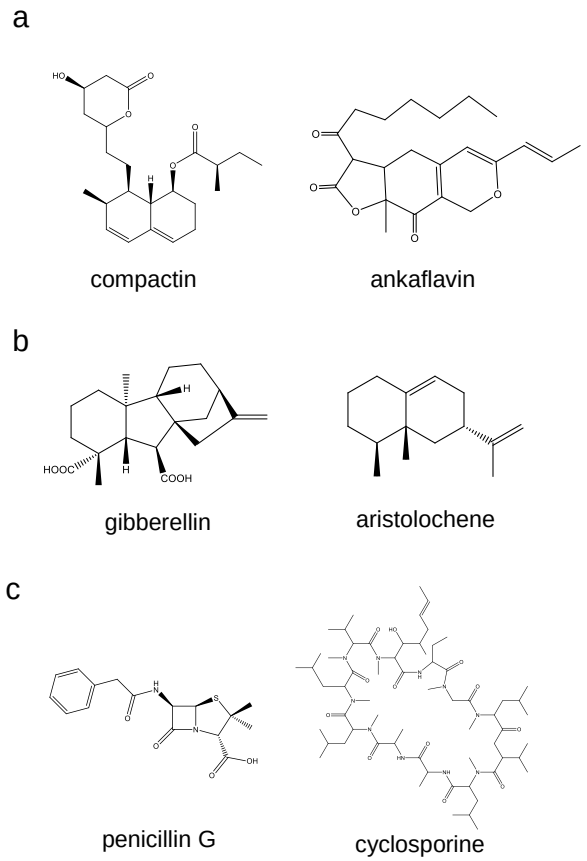

Fig. 1.3. Main group of fungal secondary metabolites. The structures of representative compounds in each group (a) polyketides, (b) isoprenoids, (c) non-ribosomal peptides.

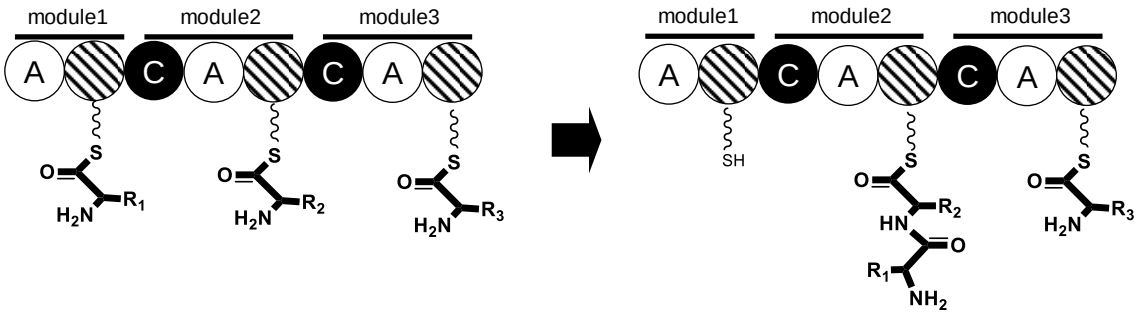

Fig. 1.4. Scheme of non-ribosomal peptide biosynthesis. The white circles labeled A represent adenylation (A) domains. The black circles labeled C represent condensation (C) domains. The hatched circles indicate peptidyl carrier protein (PCP) domains.

1.4 Entomopathogenic fungi

1.4.1 General information

Entomopathogenic fungi are classified as fungi that grow either inside of insect bodies or on the surface of their exoskeleton, the infection of which eventually cause the death of the host insect. They have a unique synchronized life cycle, interacting with their host insects. Asexual spore or conidia play an important role at the infection stage in the whole processes of the pathogenicity of entomopathogenic fungi. Firstly, germ tube emerges from asexual spore or conidia on the surface of insect exoskeleton. Then, it penetrates into insect body by mechanical presser and by secreting cuticle-degrading enzyme such as protease or chitinase. After invasion into insect body, entomopathogenic fungi proliferate in the haemolymph by vegetative growth, affecting insect's immunities by secreting secondary metabolites. Host insects eventually die because of starvation, dryness, or toxic effect caused by insecticidal secondary metabolites. Conidia or fruiting bodies are formed outside the cadaver of host insects for the succession to the future generation.

1.4.2 Relationship between entomopathogenic fungi and human

During the special life cycle which is strongly dependent on the interaction with insects, some of entomopathogenic fungi exert influence on human activities by killing beneficial insects. *Metarhizium anisopliae* and *Beauveria bassiana* are known to be a

causative agent of black muscardine disease and white/yellow muscardine disease of silk warm pupa, respectively, which do serious damage to silk producing farmers. Meanwhile, entomopathogenic fungi have been utilized for human health from ancient. One well-known species among these fungi is *Cordyceps sinensis*, and the insect complex of this species is designated as Tochu-Kaso which has been used as a traditional Chinese herbal medicine for more than 1,500 years in both China and in Japan.

Nowadays, pathogenicity of entomopathogenic fungi against insects have been reevaluated and applied for agriculture. *M. anisopliae, B. bassiana, Isaria fumosoroseus* (formerly *Paecilomyces fumosoroseus*) and species of *Lecanicillium* (formerly *Verticillium lecanii*) are well-known entomopathogenic fungi that have been commercialized and used as insecticides in place of synthetic agrochemicals all over the world (Faria and Wraight 2007). Furthermore, entomopathogenic fungi are regarded as source of bioactive compounds. Isaka et al. (2005) have continuously isolated numerous bioactive compounds possessing anti-tumor or anti-tuberculosis activities from entomopathogenic fungi collected in tropical forest in Thailand. In addition to their work, Molnár et al. (2010) introduced 89 secondary metabolites produced by entomopathogenic fungi including toxins in a review.

1.4.3 Molecular genetic study on secondary metabolism in entomopathogenic fungi

Molecular studies for secondary metabolism in entomopathogenic fungi mainly focused on the insecticidal toxins, because they have been regarded as one of the major pathogenic factors in the useful entomopathogenic fungi (Amiri et al. 1999; Bandani et al. 2000; Strasser et al. 2000). However, only a limited number of compounds have been verified as the cause of the pathogenicity, such as destruxins from *M. anisopliae*, and beauvericin and bassianolide from *B. bassiana* (Wang et al. 2012; Xu et al. 2008, 2009), due to the difficulty in establishing the transformation systems (such as for gene disruption and over-expression of biosynthetic gene) required to confirm the direct relationship between pathogenicity and the secondary metabolites. In *M. anisopliae* and *B. bassiana*, a transformation system has been well developed with the efficient and reliable *Agrobacterium*-mediated method using a glufosinate-resistance gene as the marker (Fang et al. 2004; Staats et al. 2007). In contrast, no transformation system is available in other species and only a few studies on the biosynthesis of secondary metabolites have been reported in other species of entomopathogenic fungi because of the lack of suitable transformation systems and other genetic tools.

1.4.4 *Lecanicillium* species

Lecanicillium, a genus of entomopathogenic fungi, is used as an alternative of chemicals in agricultural pest control. Among entomopathogenic fungi used

commercially as bio-pesticide, *Lecanicillium* is regarded as one of the most important genus because the genus also shows versatile activity against plant pathogenic fungi and nematode in addition to pest insect such as whiteflies and aphids. In addition to the agricultural utility, *Lecanicillium* gathers attention as a good source of novel compounds due to the productivity of secondary metabolites, as exemplified by the isolation of indolosesquiterpenes (lecanindoles A-D), phenopicolinic acid derivatives (vertilecanins) and pregnanes (Roll et al. 2009; Soman et al. 2001; Claydon et al. 1984; Grove et al. 1984).

1.5 Overview of this study

Since it was considered that detailed understanding about the secondary metabolism will be beneficial to enhance the utility of *Lecanicillium* sp., this study aimed to investigate the biosynthesis of lipopeptide compounds produced by entomopathogenic fungus *Lecanicillium* sp.. My work is divided into 4 chapters in this thesis; Chapter 2-5. In chapter 2, two lipopeptide compounds; verlamelin A and B, estimated to be present in the fermentation broth of *Lecanicillium* sp. from preliminary analysis, were isolated and structurally elucidated. Although structure of verlamelin A was reported so far, the structure was thought to be still ambiguous, since the report lacked detailed experimental data required for structure determination (Kim et al. 2002; Onishi et al. 1980; Rowin et al. 1986). Furthermore, stereochemical structure has been partially

undetermined. Therefore, in order to definitively determine the structure of verlamelin and the new derivative, precise spectroscopic analysis and chemical modifications were conducted. Although the biosynthesis of lipopeptide verlamelin was worth investigating, there was no clue to approach the biosynthetic gene(s) for the biosynthesis. Therefore, in chapter 3, host-vector system in *Lecanicillium* sp. was constructed to enable the investigation about verlamelin biosynthesis in *Lecanicillium* sp. at molecular genetic level. As for the vector, both integrating and replicating vectors were applied. Meanwhile, to make this system more efficient, gene targeting efficiency was enhanced by knocking out *ku80* gene. In chapter 4, the biosynthetic gene cluster for verlamelin biosynthesis was identified and characterized in order to investigate the biosynthetic pathway. The locus responsible for the verlamelin biosynthesis was identified by disruption of several NRPS genes. The flanking genes to NRPS genes were characterized by gene-disruption and precursor feeding studies. In chapter 5, the general conclusion of this study is given.

Chapter 2

Definitive structure determination of verlamelin

2.1 Introduction

During my investigation about secondary metabolites produced by *Lecanicillium* spp., it was found that strain HF627 produces large amount of secondary metabolites in the culture. By preliminary purification and spectroscopic analysis of them, it was suggested that the culture extract of *Lecanicillium* sp. HF627 contains verlamelin and it new derivative.

Verlamelin is a peptide antibiotic that was initially isolated from *Verticillium lamellicola* (Fig. 2.1.) (Onishi et al. 1980) and shown to exhibit antifungal activity against plant pathogenic fungi, including morphological changes to fungal cells such as swelling/bulging, or lysis (Kim et al. 2002; Rowin et al. 1986). Although the planar structure of verlamelin has already been reported, its structure determination was only preliminary, because these reports lacked detailed information on the signal assignments of $^{1}H/^{13}C$, the signal connectivity in HSQC/HMBC and the D/L configuration of the component amino acids (Kim et al. 2002; Onishi et al. 1980; Rowin et al. 1986). Furthermore, the configuration of a hydroxyl group on the 5-hydroxytetradecanoic acid moiety has not yet been determined. Therefore, in order to completely establish the structure of verlamelin, detailed structure determination of **1** and **2** as shown in Fig. 2.1 was conducted in this chapter.

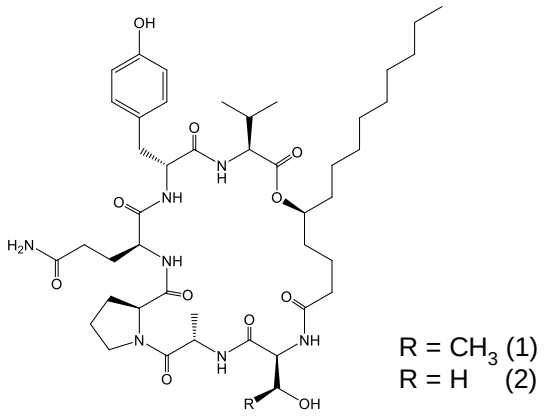

Fig. 2.1. Stereochemical structure of verlamelin A (**1**) and B (**2**), refined in this study.

2.2 Materials and methods

2.2.1 General experimental procedure

NMR spectra were recorded on a JEOL JMN-ECS400 (JEOL, Tokyo, Japan) at 400 MHz for ^{1}H and 100 MHz for ^{13}C. The ^{1}H and ^{13}C chemical shifts were referenced to the solvent signal (δH 2.49 and δC 39.5 in dimethyl sulfoxide (DMSO)-d6, δH 3.31 in CD_3OD). HRFABMS were recorded on a JEOL JMS-700 spectrometer. Optical rotation was measured on a P-1020 polarimeter (Jasco, Tokyo, Japan). The UV spectrum was recorded on a Hitachi U-3200 spectrophotometer.

2.2.2 Fungal material

The entomopathogenic fungus *Lecanicillium* sp. HF627 was isolated from a chillie thrips cadaver. Fungal conidia that had developed on the surface of the cadaver were transferred onto solid Sabouraud maltose yeast-extract (SMY) medium (4% maltose,

1% yeast extract, 1% peptone) with 1.5% agar and incubated at 25°C for several days. After several rounds of single-colony isolation, the isolated strain was identified as *Verticillium lecanii* (*Lecanicillium* sp.) according to its morphology. The fungus is deposited at the culture collection of Natural Institute of Fruit Tree Science and The National Institute of Agrobiological Sciences Genebank under strain number HF627 and MAFF 635047 respectively.

2.2.3 Fermentation and isolation

The seed culture was prepared by inoculating conidia of strain HF627 into 50 ml of SMY medium in a 500-ml baffled flask, followed by cultivation on a rotatory shaker at 28°C and 160 rpm for 3 days. For the main cultivation, the seed culture (2 ml) was inoculated into 100 ml of Medium #5 [8% sucrose, 4% yeast extract, 0.5% $CaCO_3$, 1% activated HP20 (Mitsubishi Chemical Co., Japan) by methanol] in 500-ml Erlenmeyer flasks, followed by static incubation for 21 days at 25°C. The culture broth (1 L) was mixed with *n*-butanol (500 ml) and stirred for one hour, and the *n*-butanol layer was collected after centrifugation (3000 rpm, 10 min), dried over anhydrous sodium sulfate, and concentrated *in vacuo* using a rotary evaporator, yielding 3 g of brown gum as the crude extract. The crude extract was fractionated on a silica gel 60 (70-230 mesh; Merck, Germany) column (Ø30 mm) by stepwise elution with increasing ethyl acetate concentrations (hexane/ethyl acetate = 4:1, 2:1, 3:2, 1:1, 1:2, 1:4 and 0:10 v/v), followed

by stepwise elution with increasing methanol concentrations (ethyl acetate/methanol = 40:1, 20:1, 10:1, 8:1, 4:1, 2:1, 1:1, and 0:10 v/v). Fractions containing verlamelins were detected by silica gel TLC (ethyl acetate/methanol = 2:1, Rf 0.21), combined, and evaporated *in vacuo* until dryness. The residues were further fractionated with a Sep-Pak Silica 35cc Vac cartridge (10 g; Waters, USA) by stepwise elution with increasing methanol concentrations (ethyl acetate/methanol = 2:1, 3:2, 1:1, 1:2, 1:4, and 0:10 v/v). Verlamelins in the Sep-Pak fractions were further separated by preparative reverse phase HPLC with a Shiseido Capcell-Pak C18 column (Ø10 x 250 mm) with isocratic elution using 80% methanol at a flow rate of 4 ml/min. The peaks of **2** and **1**, detected at 11 and 12 min by UV (210 nm), respectively, were collected individually, and evaporated *in vacuo* to dryness, yielding 2.7 and 65.5 mg of colorless amorphous solid, respectively.

Additional quadruplicate experiments without the Sep-Pak Silica fractionation were carried out to further obtain **2**. As a result, a total of 97.7 mg of **2** was obtained.

Compound (**1**): a colerless solid; $[\alpha]^{23}_{D}$ +2.5 (c 0.01, MeOH); UV (MeOH) λ_{max} (log ε) 224 (4.20), 278 (3.29) nm; HRFABMS m/z 886.5289 $[M+H]^+$ (calcd for $C_{45}H_{72}N_7O_{11}$, 886.5290). For ^1H, ^{13}C, see Table 2.1.

Compound (**2**): a colerless solid; $[\alpha]^{23}_{D}$ -68.5 (c 0.01, MeOH); UV (MeOH) λ_{max} (log ε) 224 (4.12), 278 (3.26) nm; HRFABMS m/z 872.5140 $[M+H]^+$ (calcd for $C_{44}H_{70}N_7O_{11}$, 872.5134). For ^1H, ^{13}C, see Table 2.1.

2.2.4 Stereochemistry of amino acids constituting verlamelin A and B

One mg aliquots of **1** or **2** were hydrolyzed by heating at 115°C for 8 hours in 10 ml of 6 M HCl. After cooling to room temperature, they were completely dried *in vacuo* and dissolved in 150 µl of water. Marfey's reagent (300 µl of 10 mg/ml solution in acetone) [N^{α}-(2,4-Dinitro-5-fluorophenyl)-L-alaninamide] (TCI, Japan) was added, followed by the addition of 70 µl of 1M $NaHCO_3$. The reactions proceeded at 37°C for one hour and were quenched by addition of 70 µl of 1 M HCl. The resulting mixture was dried *in vacuo* and then dissolved in 1 ml of DMSO to be analyzed by HPLC. Marfey's derivatives of amino acids as a standard were prepared by reacting 50 mM of amino acids in the same manner as described above. HPLC analysis was carried out on a Shiseido Capcell-Pak C18 column (Ø4.6 x 250 mm) with a linear gradient of CH_3CN from 10% to 50% in 0.05% aqueous TFA solution (60 min from 10% to 50%, 5 min at 50%, 3 min from 50% to 10%), at a flow rate of 1.0 ml/min, with detection at 340 nm. The glutamine (Gln) residues of **1** and **2** should be converted by acid hydrolysis to glutamic acid (Glu). Retention times (min) of Marfey's derivatives used as standereds were as follows: L-Ser (25.6), D-Ser (26.0), L-Thr (27.0), D-Thr (31.8), L-alloThr(27.5), D-alloThr (29.3), L-Glu (30.1), D-Glu (31.9), L-Pro (34.3), D-Pro (36.0), L-Ala (33.2), D-Ala (37.2), L-Val (42.1), D-Val (48.1), L-Tyr (57.9) and D-Tyr (40.4, 62.2).

2.2.5 (R)- and (S)-MαNP acid ester derivatives of 1 and 2

A modified Mosher's method using (R)- and (S)-MαNP acid (TCI, Japan) was used to clarify the stereogenic centers of the hydroxytetradecanoic acid moiety (Kasai et al. 2004). To protect the hydroxyl group of the Tyr residue in advance, methylation was carried out as follows. To **1** and **2** dissolved in acetonitrile (10 mg/500 µl) were added 50 µl of 1,8-diazabicyclo[5.4.0]undec-7-ene and 50 µl of CH_3I. After incubation at 50°C for 3 hours and quenching by dilution with water, the reaction products were extracted three times with an equal volume of ethyl acetate. The ethyl acetate layer was washed with 1 M HCl and brine, dried over anhydrous sodium sulfate, and concentrated *in vacuo,* yielding crude methyl ethers of **1** and **2**.

To cleave the ester linkage between hydroxytetradecanoic acid and Val residue, methanolysis was carried out as follows. Crude verlamelin methyl ethers were dissolved in 2 ml of 0.5 M methanolic sodium metoxide and stirred for 5 hours at room temperature. After quenching with 1 M HCl, extraction with ethyl acetate (equal volume, three times) and evaporation in vacuo, the cleaved product and the uncleaved reactant were collected individually by reverse phase C18 HPLC using 85% methanol as eluent. The recovered reactant was reused for the same reaction and the product was obtained as described above. The methyl ethers of **1** and **2** yielded 6.2 mg and 4.2 mg of methanolysis products, respectively.

(R)- and (S)-MαNP acid esters of **1** were prepared as follows. The methanolysis

product of **1** methyl ether (in 200 µl of CH_2Cl_2) was mixed with 2 mg of dimethyl amino pyridine, 3 mg of 1-ethyl-3-(3-dimethylaminopropyl) carbodiimide (EDC), 2 µl of triethyl amine, and 2.1 mg of (R)-MαNP acid or 2.1 mg of (S)-MαNP acid. After standing at room temperature overnight and quenching by addition of water, the reaction mixture was extracted three times with an equal volume of ethyl acetate. After washing the ethyl acetate extract with 1 M HCl and brine, drying over anhydrous sodium sulfate, and concentrating in vacuo, the (R)- and (S)-MαNP acid ester derivatives of **1** (**3**a and **3b** respectively) were purified by reverse phase HPLC on a Shiseido Capcell-Pak C18 column (Ø10 x 250 mm) with isocratic elution using 90% methanol as a mobile phase. (R)- and (S)-MαNP acid ester derivatives of **2** (**4a** and **4b** respectively) were synthesized and purified in a similar manner as those of **1**.

Compund **3a**: HRFABMS m/z 1144.6558 $[M+H]^+$ (calcd for $C_{61}H_{90}N_7O_{14}$, 1144.6546). For ^1H, see Table 2.2.

Compund **3b**: HRFABMS m/z 1144.6543 $[M+H]^+$ (calcd for $C_{61}H_{90}N_7O_{14}$, 1144.6546). For ^1H, see Table 2.2.

Compund **4a**: HRFABMS m/z 1112.6274 $[M+H]^+$ (calcd for $C_{60}H_{86}N_7O_{13}$, 1112.6283). For ^1H, see Table 2.2.

Compund **4b**: HRFABMS m/z 1112.6284 $[M+H]^+$ (calcd for $C_{60}H_{86}N_7O_{13}$, 1112.6283). For ^1H, see Table 2.2.

2.2.6 Antifungal assay

In vitro antifungal activity of **1** and **2** against *Cladosporium cucumerinum* was tested by disc diffusion method as follows. Loaded paper discs (1, 0.5, 0.25, 0.125 μg/disc by 10 μl of DMSO solution) was placed on the potato dextrose agar (PDA) medium (Difco) inoculated with conidia of *Cladosporium cucumerinum* NBRC6370 (10^6 conidia/ml). Growth inhibitory effect was observed after 4 days of incubation at 28℃.

2.3 Results and discussion

Lecanicillium sp. HF627 was cultivated under static conditions in liquid medium containing sucrose 8%, yeast extract 4%, $CaCO_3$ 0.5% and HP20 1%. The whole broth was extracted with *n*-butanol. Compound **1** and **2** were purified by series of steps with silica gel column chromatography, C18 column chromatography and preparative reverse phase HPLCs.

Both major compound **1** and minor compound **2** were obtained as colorless solid. The molecular formula of **1** was identified as $C_{45}H_{71}N_7O_{11}$ based on high-resolution fast atom bombardment mass spectrometry (HRFABMS) (obs. m/z 886.5289 $[M+H]^+$, calcd 886.5290 for $C_{45}H_{72}N_7O_{11}$). The molecular formula of **2** was $C_{44}H_{69}N_7O_{11}$ (HRFABMS, obs. m/z 872.5140 $[M+H]^+$, calcd 872.5134 for $C_{44}H_{70}N_7O_{11}$), suggesting that **2** is a one-methylene-shorter derivative of **1**, considering the almost identical UV/Vis spectrum (λ_{max} 224, 278 nm).

All the ^{13}C signals and all the ^{1}H signals were assigned using DEPT135, HSQC, COSY and HMBC (Table 2.1). ^{13}C NMR of the two compounds detected eight carbonyl carbons in the range of δ_C 170-174, and ^{1}H NMR in DMSO-d_6 revealed 8 broad resonances which were not detectable in the measurement using methanol-d_4, suggesting that certain numbers of amide linkages were present in these compounds. Overlapping methylene signals in the high magnetic field suggested that both compounds have an alkyl chain. Based on these data, **1** and **2** were assumed to bear typical lipopeptide substructures. By COSY and HMBC correlations, the component amino acids were estimated to be valine (Val), alanine (Ala), tyrosine (Tyr), threonine (Thr) (**1**) or serine (Ser) (**2**), glutamine (Gln) and proline (Pro). The remaining substructure was deduced to be a 5-hydroxytetradecanoic acid moiety by comparison of the δc values of C-2 to C-6 with those on cordycommunin, which has the 5-hydroxytetradecanoic acid substructure (Haritakun et al. 2009). Since δ_H of the oxymethine H-5 was detected relatively downfield [4.79 (**1**), 4.77 (**2**)], the C-5 was judged to be involved in ester bonding. The connecting sequence of components was finally determined as 5-hydroxytetradecanoic acid, Thr (**1**) or Ser (**2**), Ala, Pro, Gln, Tyr, and Val, based on HMBC and ROESY (**1**), NOESY (**2**) correlation. HMBC correlation of the oxymethine on 5-hydroxytetradecanoic acid with C-1 on Val demonstrated the formation of a cyclic structure (Fig. 2.2). Thus, the compound **2** was proposed to be a new analog of verlamelin (verlamelin B) in which Ser was replaced with Thr.

To determine the absolute configurations in the peptide moiety of the verlamelins, Marfey's analysis was conducted (Bhushan et al. 2004). After degradation of verlamelin A and verlamelin B under acidic conditions, the hydrolysate was labeled by Marfey's reagent [Nα-(5-Fluoro-2,4-dinitrophenyl)-L-alaninamide]. The retention times of the labeled products in C18 HPLC (29.3, 30.2, 34.5, 37.3, 40.4, 42.1, 62.2 min for verlamelin A; and 26.0, 30.2, 34.6, 37.3, 40.5, 42.2, 62.2 min for verlamelin B) indicated that the component amino acids were L-Gln, L-Pro, D-Ala, L-Val, D-Tyr and D-allo-Thr (verlamelin A) or D-Ser (verlamelin B) (see Materials and methods for standards).

As for the absolute configuration of C-5 in the 5-hydroxytetradecanoic acid moiety, a modified Mosher's method was employed (Kasai et al. 2004; Kusumi et al. 2005). After the reactive phenolic hydroxyl group was protected by methyl iodide and the macrolactone ring was cleaved by methanolysis, the reaction products (purified by C18 HPLC) showed m/z at 932.5 and 918.5, respectively, suggesting that methanolysis proceeded successfully. Reaction of the product from **1** with (R) or (S)- MαNP acid (M.W.: 230.2) gave products (purified by C18 HPLC) of m/z at 1144.6, implying that the esterification with MαNP occurred at a single position. Similar esterification reaction of the product from **2** gave products of m/z 1342.7, suggesting that the two molecules of MαNP were incorporated. Subsequent partial hydrolysis with K_2CO_3 resulted in the loss of one MαNP at the primary alcohol of the Ser residue, and yielded a

product of m/z at 1112.6, corresponding to the monoester with an MαNP. Each monoester with an MαNP was analyzed by ^{1}H NMR and COSY to observe the anisotropic effect as the result of shielding by the MαNP group. The Δδ (δR-δS) values of the Mosher's esters indicated the 5-S configuration (Fig. 2.2). Based on these results, the absolute structures of verlamelin A and verlamelin B were definitively determined for the first time, as shown in Fig. 2.1.

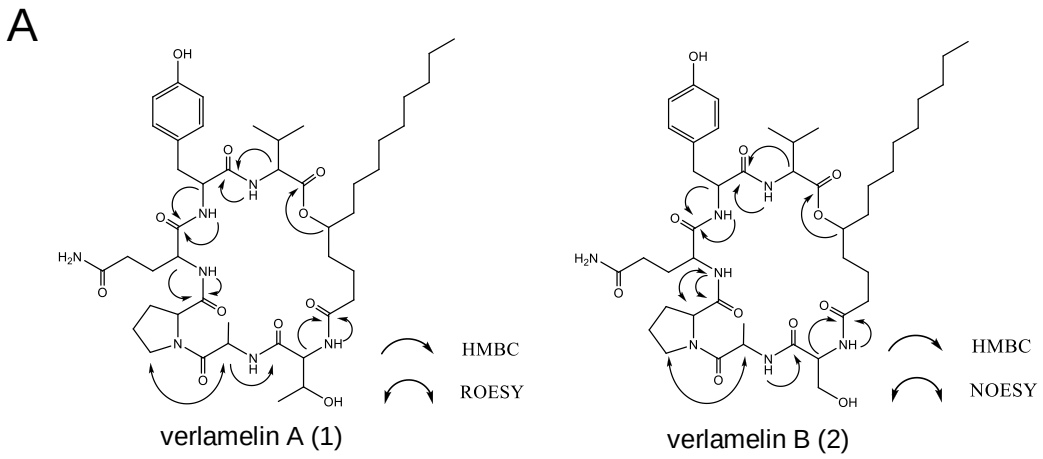

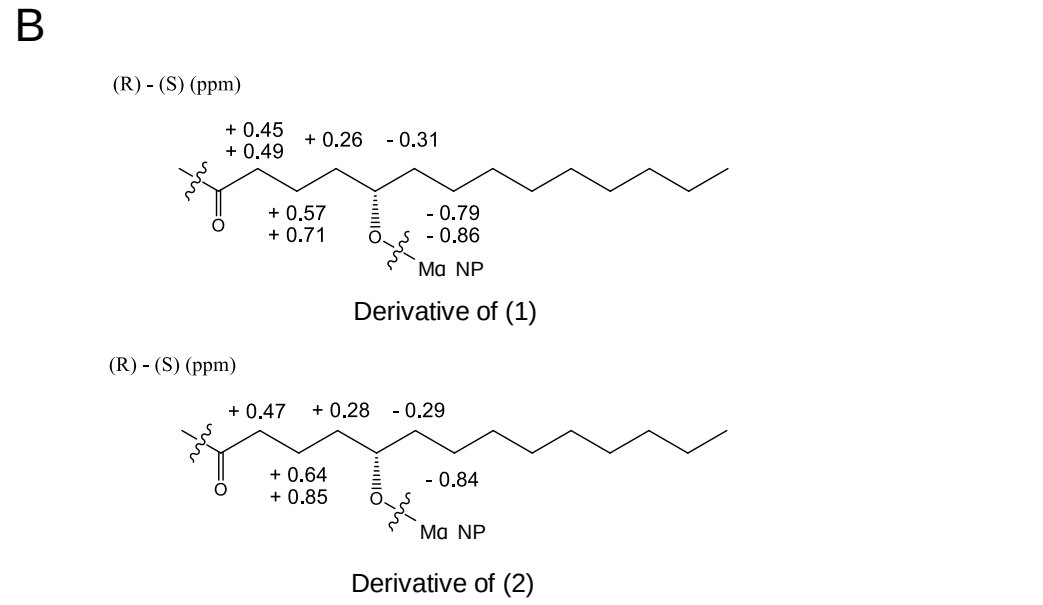

Fig. 2.2. Structure analysis of verlamelins. (A) Key HMBC, ROESY (1) and NOESY (2) correlation. (B) Partial (R) – (S) values of derivatives of (1) and (2) synthesized by a modified Mosher's method.

Table 2.1 NMR Spectroscopic data (400 MHz, DMSO-d6) for verlamelin A (**1**) and verlamelin B (**2**)

verlamelin A (**1**)			verlamelin B (**2**)		
Position	δC, mult.	δH, mult. (*J* in Hz)	Position	δC, mult.	δH, mult. (*J* in Hz)
	L-Val			L-Val	
1	170.8, qC	-	1	170.8, qC	-
2	59.4, CH	3.84, t (7.3)	2	59.3, CH	3.86, t (7.3)
3	29.2, CH	1.91-2.04,[b] m	3	29.2, CH	1.97-2.02,[i] m
4	18.5, CH3	0.82, d (6.4)	4	18.5, CH3	0.81, d (6.4)
4’	19, CH3	0.84, d (6.4)	5	19, CH3	0.84, d (6.4)
NH	-	8.46, bd (6.9)	NH	-	8.41, bd (6.9)
	D-Tyr			D-Tyr	
1	172.7, qC	-	1	172.5, qC	-
2	54.2, CH	4.61, m	2	54.0, CH	4.64, m
3	38.0, CH2	2.75, m	3	38.1, CH2	2.73, m
4	127.5, qC	-	4	127.5, qC	-
5, 9	130.3, CH	7.04, d (8.7)	5, 9	130.3, CH	7.02, d (8.2)
6, 8	114.8, CH	6.60, d (8.7)	6, 8	114.8, CH	6.59, d(8.2)
7	155.8, qC	-	7	155.8, qC	-
7-OH	-	9.09, bs	7-OH	-	9.11, bs
NH	-	7.50, bd (9.6)	NH	-	7.55, bd (8.1)
	L-Gln			L-Gln	
1	171.0, qC	-	1	170.9, qC	-
2	52.7, CH	4.04, m	2	52.6, CH	4.09, m
3	26.8, CH2	1.71, m; 1.91-2.04,[b] m	3	27.1, CH2	1.71, m; 1.89, m
4	31.8, CH2	1.91-2.04,[b] m	4	31.8, CH2	1.97-2.02,[i] m
CONH2	173.7, qC	6.74, bs; 7.21, bs	CONH2	173.8, qC	6.74, bs; 7.21, bs
NH	-	7.78, bd (8.2)	NH	-	7.75, bd (8.2)
	L-Pro			L-Pro	
1	170.9, qC	-	1	171.0, qC	-
2	60.2, CH	4.33, m	2	60.1, CH	4.33, m
3	29.2, CH2	1.83-1.84,[d] m; 2.11-2.16,[c] m	3	29.2, CH2	1.81,[j] m; 2.09, m
4	24.2, CH2	1.83-1.84,[d] m	4	24.2, CH2	1.81,[j] m
5	46.8, CH2	3.48, m; 3.62, m	5	46.7, CH2	3.45, m; 3.54, m
	D-Ala			D-Ala	
1	171.0, qC	-	1	170.6, qC	-
2	46.9, CH	4.48, m	2	47.0, CH	4.48, m
3	16.3, CH3	1.18, d (6.4)	3	16.2, CH3	1.15, d (6.4)
NH	-	7.80, bd (6.4)	NH	-	7.76, bd (6.4)
	D-allo-Thr			D-Ser	
1	170.5, qC	-	1	170.6, qC	-
2	58.3, CH	4.20, dd (7.1, 8.7)	2	55.3, CH	4.27, m
3	66.4, CH	3.99, m	3	61.3, CH2	3.64, m
4	20.0, CH3	1.08, d (6.4)	3-OH	-	5.27, bt (4.6)
3-OH	-	5.27, bs	NH	-	7.63, bd (7.7)
NH	-	7.48, bd (9.2)			
	5(S)-hydroxytetradecanoic acid			5(S)-hydroxytetradecanoic acid	
1	172.2, qC	-	1	172.6, qC	-
2	34.7, CH2	1.91-2.04,[b] m; 2.11-2.16,[c] m	2	34.3, CH2	1.97-2.02,[i] m; 2.21, m
3	19.8, CH2	1.33-1.35,[e] m	3	19.8, CH2	1.33-1.37,[k] m
4	32.7, CH2	1.33-1.35,[e] m; 1.42-1.46,[f] m	4	32.6, CH2	1.33-1.37,[k] m; 1.42-1.44,[l] m
5	73.2, CH	4.79, m	5	73.2, CH	4.77, m
6	33.5, CH2	1.42-1.46,[f] m	6	33.6, CH2	1.42-1.44,[l] m
7	25.0, CH2	1.20-1.23,[g] m	7	24.9, CH2	1.20-1.23,[m] m
8	29.0,[a] CH2	1.20-1.23,[g] m	8	29.0,[h] CH2	1.20-1.23,[m] m
9	28.9,[a] CH2	1.20-1.23,[g] m	9	28.9,[h] CH2	1.20-1.23,[m] m
10	28.7,[a] CH2	1.20-1.23,[g] m	10	28.7,[h] CH2	1.20-1.23,[m] m
11	28.7,[a] CH2	1.20-1.23,[g] m	11	28.7,[h] CH2	1.20-1.23,[m] m
12	31.3, CH2	1.20-1.23,[g] m	12	31.3, CH2	1.20-1.23,[m] m
13	22.1, CH2	1.20-1.23,[g] m	13	22.1, CH2	1.20-1.23,[m] m
14	14.0, CH3	0.83, t (6.9)	14	14.0, CH3	0.83, t (6.9)

[ah]Carbon chemical shifts may be interchanged. [bcdefgijklm]The proton resonances are overlapped.

Table 2.2. ^{1}H NMR Spectroscopic data (400 MHz, CD_3OD) of MαNP ester **1** (**3a**, **3b**) and **2** (**4a**, **4b**).

Position	δ_H, mult.			
	(R)-MαNP ester **1** (**3a**)	(S)-MαNP ester **1** (**3b**)	(R)-MαNP ester **2** (**4a**)	(S)-MαNP ester **2** (**4b**)
	5-hydroxytetradecanoic acid		5-hydroxytetradecanoic acid	
1	-	-	-	-
2	2.21, m	1.72, m; 1.76, m	2.21, m	1.74, m
3	1.45,[b] m; 1.55, m	0.74, m; 0.98, m	1.53, m	0.68, m; 0.89, m
4	1.45,[b] m	1.1-1.3,[d] m	1.45, m	1.1-1.3,[f] m
5	-[a]	-[a]	-[a]	-[a]
6	1.09, m	1.40, m	1.08, m	1.39, m
7	0.30, m; 0.37, m	1.1-1.3,[d] m	0.33, m	1.1-1.3,[f] m
8	0.67, m	1.1-1.3,[d] m	0.69, m	1.1-1.3,[f] m
9	0.75, m	1.1-1.3,[d] m	0.77, m	1.1-1.3,[f] m
10	1.00, m	1.1-1.3,[d] m	1.00, m	1.1-1.3,[f] m
11	1.20,[c] m	1.1-1.3,[d] m	1.20,[e] m	1.1-1.3,[f] m
12	1.20,[c] m	1.1-1.3,[d] m	1.20,[e] m	1.1-1.3,[f] m
13	1.31, m	1.29, m	1.30, m	1.31, m
14	0.91, t	0.89, t	0.91, t	0.90, t

[a]The proton resonances were not observed provably because of overlapping with the resonances of H_2O at 4.84 ppm.

[bcdef]The proton resonances are overlapped.

Since in vitro antifungal activity of verlamelin was previously reported (Onishi et al. 1980; Kim et al. 2002; Rowin et al. 1986), we measured the antifungal activity of **1** and **2** by disc diffusion method. The new derivative of verlamelin, **2,** showed potent activity against *Cladosporium cucumerinum* (0.5 µg/disc), while it was slightly less active than **1** (0.25 µg/disc).

By detailed structure determination, the absolute structures of **1** and **2** were found to consist of a cyclic lipodepsipeptide, cyclo(5S-hydroxytetradecanoic acid-D-alloThr/Ser-D-Ala-L-Pro-L-Gln-D-Tyr-L-Val) (Fig. 2.1). The related compounds were W493 A/B, cyclo(3S-hydroxy-4R-methyltetradecanoic acid-D-alloThr-L-Ala-D-Ala-L-Gln-D-Tyr-L-Val/Ile), isolated from *Fusarium* sp. (Nihei et al. 1998), and cordycommunin, cyclo(5-hydroxytetradecanoic acid-D-alloThr-L-Ala-L-Ala-L-Gln-L-Tyr-L-Val), isolated from *Ophiocordyceps communis* (Haritakun et al. 2009). These compounds share several common features, including the arrangement of amino acids in their peptidyl structures, hydroxylated fatty acid moieties of C14 chain length, and macro-cyclic structures with ester bonding between the hydroxyl group on the fatty acid moiety and C-terminal aliphatic amino acid. The configuration of hydroxyl group on fatty acid moiety of **1** and **2** were same as that of W493 A/B, both of which were S-configuration.

2.4 Summary

In this chapter, isolation and structure determination of verlamelin and its newly discovered derivative produced by entomopathogenic fungus *Lecanicillium* sp. was conducted to determine their absolute structure, which have not been analyzed so far even in verlamelin, reported compound. Verlamelin and its new derivative were isolated by series steps of purification, and the planer structures of which were determined by NMR and HRFABMS analysis, revealing that new derivative of verlamelin has Ser moiety instead of Thr on verlamelin. The configuration on the entire stereogenic center of both compounds was determined by application of Marfey's method and modified Mosher's method. As a result, the absolute structures were definitively determined to be cyclo(5S-hydroxytetradecanoic acid-D-alloThr/Ser-D-Ala-L-Pro-L-Gln-D-Tyr-L-Val). Verlamelin and its new derivative were renamed as verlamelin A and verlamelin B respectively, since this is the first study precisely determining the structure of these compounds.

Chapter 3

Construction of efficient and versatile transformation system in *Lecanicillium* sp. HF627

3.1 Introduction

Species of *Lecanicillium* are utilized as bioinsecticides against aphid and white fly, both of which are serious pest insects in greenhouses. In addition, these species have been a focus of attention because of their potential as biopesticides against both plant parasitic nematodes and plant pathogenic fungi (Benhamou 2004; Kim et al. 2007; Meyer and Meyer 1996; Nguyen et al. 2007). However, despite of these utility, suitable molecular genetic techniques have not been established while transformation by protoplast method was reported with nitrate reductase gene as a marker (Hasan et al. 2011).

Efficient genetic studies are often hampered in filamentous fungi due to the dominancy of ectopic integration by vector DNA during the transformation via non-homologous end-joining (NHEJ), which is one of the pathways for repairing broken double-strand DNA in eukaryotes (Pastink et al. 2001). At least six proteins are required for NHEJ (Ku70, Ku80, DNA-PKcs, Artemis, XRCC4 and DNA ligase IV) (Meek et al. 2004). The Ku70-Ku80 heterodimer binds to the end of a DNA double-strand break, forming a DNA-PK complex with DNA-PKcs, which interacts with the DNA end-processing nuclease Artemis and XRCC4-DNA ligase IV complex (Hsu et al. 2002). The repair of broken DNA is accomplished via the direct ligation of

DNA by the XRCC4-DNA ligase IV complex. Since NHEJ is predominant to homologous recombination in filamentous fungi, the frequency of homologous recombination is very low, which hampers the genetic analysis through gene targeting, versus the case in yeast *Saccharomyces cerevisiae*, where homologous recombination is predominant to NHEJ. (Bird et al. 1997; Takita et al. 1997).

In this chapter, an efficient and versatile host-vector system for genetic study in the *Lecanicillium* sp. HF627 strain was constructed, to make a basis for genetic studies of secondary metabolism in this strain. A transformation system using a uridine auxotrophic strain and an endogenous *pyrG* gene was constructed. To improve the utility of this system, an autonomously replicating vector harboring the AMA1 sequence from *Aspergillus nidulans* (Gems et al. 1991) was adopted. Finally, a useful host strain which showed a much lowered frequency of non-target integration was successfully constructed, by knocking out the *ku80* gene and by deleting endogenous *pyrG*, which was homologous to the marker gene.

3.2 Materials and methods

3.2.1 Fungal strain and media

Lecanicillium sp. HF627, isolated from a cadaver of chilli thrips, was used as a wild-type strain. Conidia were collected after growth on potato dextrose agar (PDA) medium (Difco), which was supplemented with 10 mM uridine as required. CD^{+}

medium, which was used for the auxotrophic study, was prepared by the addition of 0.2% $(NH_4)_2SO_4$ to Czapek-Dox (CD) medium (Oxoid, Hampshire, UK) (with 1.5% of agar for plate).

3.2.2 Cloning of the *pyrG* gene

The *pyrG* gene encoding orotidine-5'-phosphate (OMP) decarboxylase was selected as a uridine auxotrophic marker in HF627. Internal fragments of *pyrG* (797, 804 and 903 bp) were amplified by PCR using degenerate primer sets (pyrg1-pyrg4, pyrg2-pyrg3, and pyrg2-pyrg4, respectively; Table 3.1) designed from the conserved regions. A partial genomic library was prepared in *E. coli* DH5α by ligating *Bam*HI/*Sph*I-digested genomic fragments with pUC19. Colony PCR screening was performed using a primer set (pyrgA-pyrgB) designed based on the sequence of the internal fragments.

3.2.3 Plasmids

A plasmid containing *pyrG* in pUC19 (pLSPYRG) was used as an integrating vector. For construction of an autonomous replication vector, an AMA1 sequence (an autonomous replicating sequence of *A. nidulans* origin) was recovered from pAUR316 (Takara) by *Sma*I/*Bam*HI-digestion, and subcloned into *Sma*I/*Bam*HI-digested pUC19, followed by cloning of the *Bam*HI/*Sph*I fragment containing the entire *pyrG*, yielding

pLSPTRGAT.

3.2.4 Uridine auxotrophic mutant strain

The uridine auxotrophic strain Ki6 (*pyrG*$^{-}$) was obtained by the UV mutagenesis and filter-enrichment method described by Nagashima et al. (1994) with several modifications. A conidia suspension of the wild-type strain HF627 (10 ml, 6 x 10^7 to 1 x 10^8 conidia/ml) in a Petri dish was irradiated by UV (15 W) for 15 min with an irradiation distance of 60 cm. The mutated conidia were incubated with shaking (28ºC, 160 rpm, 12 h) in a 500 ml-baffled flask containing 100 ml of Czapek-Dox liquid media supplemented with 0.2% of casamino acid. Germinated wild-type prototrophic conidia were removed by filtration with a G1 glass filter (pore size: 100-120 μm), and ungerminated conidia in the filtrate were collected by centrifugation (1,710 x *g*, 10 min). After two rounds of the germination/filtration enrichment, ungerminated conidia were spread on CD^+ plates containing 1 mg/ml of 5-fluoroorotic acid (5-FOA) and 10 mM uridine. The emerged colonies were transferred onto fresh selective medium, and tested for their uridine auxotrophy on CD^+ medium plates. The mutation in the *pyrG* gene in the uridine auxotrophic strains was identified by sequencing.

3.2.5 Transformation of *Lecanicillium* sp. HF627

Lecanicillium strains were transformed by a protoplast-polyethylene glycol (PEG)

method as previously described for *M. anisopliae* (Singkaravanit et al. 2010_b) with several modifications. The strain Ki6 (1-2 x 10^8 conidia) was inoculated and cultivated in YES medium (8% sucrose, 4% yeast extract) containing 10 mM uridine (160 rpm, 28ºC, 24 h). Germinated conidia were collected with a G1 glass filter, suspended in protoplast formation buffer [10 mM MES buffer (pH 6.0 with KOH), 1.2 M KCl, 10 mg/ml Yatalase (Takara) and Lysing enzyme (Sigma)], and incubated for 4 h at 30ºC with gentle shaking. After the removal of mycelia by cotton filtration, protoplasts were collected by a G1 glass filter, washed with enzyme-free protoplast formation buffer, and suspended in TF Solution 1 [1.2 M KCl and 10 mM $CaCl_2$ in 10 mM Tris-HCl (pH 8)] to a concentration of 1-2 x 10^8/ml. An aliquot of the protoplast suspension (200 μl) was mixed with DNA solution (10 μl, 2 μg/μl), followed by the addition of 20 μl of TF Solution 2 [60% polyethylene glycol and 10 mM $CaCl_2$ in 10 mM Tris-HCl (pH 8)]. The mixture was kept on ice for 30 min, followed by an additional 10 min incubation at room temperature after the addition of 1 ml TF Solution 2. The transformed protoplast mix was washed with TF Solution 1, and suspended in CD^+ soft agar (0.8% agar containing 0.8 M KCl) and spread on CD^+ agar containing 0.8 M KCl. The plate was incubated at 25ºC for 6 to 10 days until colonies emerged.

3.2.6 *ku80* knock-out

A portion of the *ku80* homologous gene was prepared for use as a probe by PCR

with a degenerate primer set designed from conserved amino acid sequences of fungal Ku80 (ku2-ku4, Table 3.1). The entire *ku80* gene was obtained by colony PCR (primers ku81-ku82; Table 1) from the *Eco*RI-partial genomic library prepared with pUC19.

A mutated *ku80* gene containing a nonsense mutation was prepared by fusion PCR (ku8mN1-ku8mN2 and ku8mC1-ku8mC2 for the first-round PCR, and ku8mN1-ku8mC2 for the second-round PCR) and cloned into *Bam*HI/*Sac*I-digested pLSPYRG, yielding the transformation plasmid pKU80MUT.

To obtain *ku80*$^{-}$ strains (Fig. 3.3a), pKU80MUT-integrated clones were screened by PCR (primer sets, ku80mtckN1-ku80mtckN2, ku80mtckC1-ku80mtckC2) with an FTA® classic card (Whatman®). To confirm the pKU80MUT-integration at the correct locus, the *Eco*RI-digested genomic DNA of the candidates were analyzed by Southern hybridization with a whole *ku80* fragment (primer set, ku8mN1-ku8mC2). Conidia of the correct transformants were spread on the CD^{+} medium containing 10 mM uridine and 1 mg/ml of 5-FOA to remove the integrated vector DNA by intra-molecular second crossover. The strain having the non-sense mutation on the *ku80* locus was named Ki50c (*pyrG*$^{-}$ *ku80*$^{-}$) and was used for further study as the *ku80* knock-out strain.

3.2.7 Deletion of the *pyrG* locus

To delete the endogenous nonfunctional *pyrG* locus because its presence causes

undesired recombination with the *pyrG* marker gene on the transformation plasmid (Fig. 3.4a, b), a 4.1 kbp-fragment containing a part of *pyrG* together with its 5' flanking region was obtained by colony PCR from the *Pst*I-digested partial genomic library (in pUC19) using a primer set (pyrgN-ki627awt). A 3.1 kbp-fragment of the *pyrG* upstream region prepared by *Xba*I/*Hin*dIII-digestion of the plasmid was cloned into the *Xba*I/*Hin*dIII sites of pLSPYRG in place of the 1.3 kbp-upstream fragment, resulting in pUC19 harboring a 6.4 kbp-*pyrG* fragment containing 3.7 kbp-upstream sequence (pLSPYRGEXT). Finally, the *pyrG* disruption vector pPYRGDEL was constructed by inserting the 0.4 kbp-*pyrG* downstream region (PCR amplified with the primers pyrgdel1-pyrgdel2) into the *Sph*I site present at 1.9 kbp-upstream from the start codon of *pyrG* in pLSPYRGEXT. *Hin*dIII-digested pPYRGDEL or a PCR-fragment using pPYRGDEL as the template with primers (M13fw-pyrgB) was used for transformation as the linearized DNA.

Desired first-crossover clones, in which the artificially inserted 0.4 kbp-*pyrG* downstream region is present in the *pyrG* upstream region, were selected by PCR (a primer set, pyrGNck-pyrgdel2) with an FTA® classic card, and the genotype was confirmed by Southern hybridization using a PCR-fragment (a primer set, pyrgA-pyrgB) as the probe. Conidia of the selected transformants were spread on the CD^{+} medium containing 10 mM uridine and 5-FOA (1 mg/ml) to facilitate the intra-molecular recombination between the two 0.4 kbp-regions flanking the entire

pyrG. The emerged colonies were tested for their uridine auxotrophy, and the genotype was confirmed by Southern hybridization. Southern hybridization was performed against *Pst*I-digested genomic DNA using a *pyrG* 3'-homologous sequence as the probe. The constructed strain was designated Ki2p (*ΔpyrG ku80*$^{-}$) and was used for further study.

3.2.8 Efficiency evaluation of homologous recombination in the *ku80* mutant

The draft genome sequence of HF627 was searched for the *trp1* gene and *his3* gene by using the amino acid sequence of Trp1 and His3 from *Saccharomyces cerevisiae*, respectively. The *trp1* disruption plasmid was constructed by inserting a PCR-amplified, 1,500 bp sequence from each of the *trp1* 5' and 3' regions (primer sets, trp1N1-trp1N2 and trp1C1-trp1C2, respectively) into the *Kpn*I-*Bam*HI sites and *Sph*I-*Hin*dIII sites of pLSPYRG, respectively. The resulting plasmid contained the whole *trp1* gene interrupted by *pyrG*. The *his3* disruption plasmid was constructed in a similar fashion by inserting a PCR-amplified, 1,500 bp sequence from each of the *his3* 5' and 3' regions at the *Sph*I-*Hin*dIII sites and *Kpn*I-*Bam*HI sites, respectively, while the internal 95 nucleotides were removed. Both disruption vectors were linearized by *Hin*dIII-digestion and used for the transformation. Trp or His auxotrophy was tested on the transformants, and the auxotroph was judged to be a *trp1* or *his3* disruptant as a result of the homologous recombination.

Table 3.1. Oligonucleotides used in this chapter

Name	Sequence (5'-3')
pyrg1	GGAATTCTAGATHTTYGARGAYMGNAA
pyrg2	GGAATTCTAGAGTNGTNYTNAARACNCA
pyrg3	GGAATTCTAGAGTNTKRTAYTGYTGNCC
pyrg4	GGAATTCTAGACKRTANCKYTCNGCYTC
pyrgA	AGCGGGTCAGCCAGAATTAT
pyrgB	CACCATTCTTTCCTTCGTCG
ku2	GGAATTCTAGATWYSARTAYGGNMGNAC
ku4	GGAATTCTAGARTCYTCNKCRAANGG
ku81	GCACGGCTGTTCATATCA
ku82	GAACGGTTCGTACTGCAT
ku8mN1	GGGAGCTCGGAGTGAGTATTTGTTA
ku8mN2	TTGTAAGGCTAGACCGATTT
ku8mC1	AAATCGGTCTAGCCTTACAA
ku8mC2	GGGGATCCTCTTACATGCGCAATAT
ku80mtckN1	TTTCCACAGACTGTTCA
ku80mtckN2	TACGACTTGTAAGGCTA
ku80mtckC1	TCGCGTCAAATCGGTCT
ku80mtckC2	ACTGCGCCAACAGCAAA
pyrgN	ATTTCTGTCCAAGCGCCT
ki627awt	CCAATCTTATCGGCAAAG
pyrgdel1	GGGCATGCGGATCCAGAGTTGAGG
pyrgdel2	GGGCATGCCGATTTCTTG
M13fw	GTAAAACGACGGCCAGT
pyrGNck	TCACATCAAGGTGTGCA
pyrGCck	CATCTTCCTCCTTCGTT
trp1N1	TGGGTACCTGTGCCGCACTGTGAGC
trp1N2	AGGGATCCTTGACAGCTATCGTCA
trp1C1	TGGCATGCTTGGCTCCAAGGCCATT
trp1C2	AACAAGCTTCTTGAAACTCGACCAT
his3N1	ATAAAGCTTAATAGGAGCTTGTGTTG
his3N2	CGGCATGCCTGGGCAAAGCTCTGA
his3C1	GTGGATCCTGCCACTACGAGAGTC
his3C2	GCGGTACCTGTCAGCTTCAGTCGA

3.3 Results

3.3.1 Cloning of *pyrG* from *Lecanicillium* sp. HF627

For use as the auxotrophic marker in transformation, *pyrG* encoding orothidine 5'-phosphate (OMP) decarboxylase in pyrimidine biosynthesis was selected, and internal 797, 804 and 903 bp fragments were obtained from the genomic DNA of *Lecanicillium* sp. HF627 by PCR with degenerate primers (primers, pyrg1-pyrg4, pyrg2-pyrg3, and pyrg2-pyrg4, respectively; Table 3.1), revealing high similarity (74-95%) to fungal *pyrG*. The entire *pyrG* was obtained on a 4.6 kbp-*Bam*HI/*Sph*I fragment by screening a genomic library with primers designed from the obtained internal fragment. The *pyrG* ORF (KF147802) was 1,101 n.t. encoding a 366 amino acid protein which showed the highest similarity (96%) to OMP decarboxylase of *Cordyceps militaris* (EGX91099).

3.3.2 Generation of the uridine auxotrophic strain

To generate a *pyrG*$^{-}$ strain to serve as the host, UV-mutagenesis was conducted against strain HF627. Thirteen strains were selected that showed resistance against 5-fluoroorotic acid (5-FOA), from which six uridine auxotrophs were obtained. To identify the mutation in *pyrG*, the *pyrG* genes of the 6 uridine auxotrophs were sequenced, and the sequence in the strain Ki6 (*pyrG*$^{-}$) was found to have a single substitution from C_{153} to A_{153}, changing Tyr to a stop codon at the 51st aa.

3.3.3 Transformation system with strain Ki6 (*pyrG*$^{-}$) using an integrating plasmid

The Ki6 strain was transformed by the protoplast-PEG method (see Materials and Methods) using pLSPYRG harboring *pyrG* from HF627 as the selection marker. After six to ten days, colonies emerged on the medium without uridine, while no colony was observed in the control transformation in which no plasmid was included, indicating that uridine auxotrophy of the Ki6 strain was complemented by the introduction of the exogenous *pyrG* gene. As a result of quadruplicated experiments, the transformation efficiency was estimated to be 0.21 CFU/μg DNA. In each experiment, 3, 1, 15 and 14.4 colonies on average were obtained when normalized by 200 μl of protoplast solution.

To confirm the genotype of the transformants, Southern hybridization was conducted with a part of *pyrG* as the probe (see Materials and Methods, Fig. 3.1). Four out of the five transformants demonstrated additional signals other than the endogeneous *pyrG*, indicating that the introduced DNA was successfully integrated into the chromosome (Fig. 3.1). The signals of the same size (5.6 kbp) as the digested vector were from the vector incorporated into the *pyrG* locus by homologous recombination, while the signals of different sizes were likely from random insertion of the DNA introduced on the chromosome.

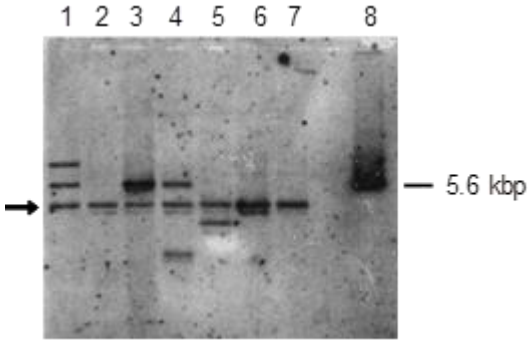

Fig. 3.1. Southern hybridization analysis of transformants after the *pyrG* gene introduction. Lanes 1 to 5, candidate transformants; lane 6, Ki6 strain (*pyrG*$^{-}$); lane 7, HF627 strain (wild-type); lane 8, pLSPYRG (signal, 5.6 kbp). Genomic DNAs were digested with *Pst*I. The band with an arrow (4.1 kbp) corresponds to the endogenous *pyrG* gene.

3.3.4 Transformation system using autonomously replicating plasmid

To increase the utility of the transformation system in *Lecanicillium*, a plasmid harboring the autonomously replicating sequence AMA1 from *A. nidulans* was used. pLSPYRGAT restored the uridine auxotrophy with an efficiency of 3.5 CFU/μg DNA, which was 16.7-fold higher than that of the integrating plasmid pLSPYRG. An expected band of 13.2 kbp corresponding to the *Bam*HI-digested pLSPYRGAT was detected by Southern hybridization from transformants grown in selective medium (Fig. 3.2a, lanes 1, 2, 5, 6 and 8), while no such band was detected when the transformants were grown in non-selective medium (Fig. 3.2b), indicating that pLSPYRGAT autonomously replicated under the selective conditions but segregated quickly without the selection pressure. Although it fluctuated among transformants, the intensity of the band corresponding to pLSPYRGAT was stronger than the signal from endogenous *pyrG*,

suggesting that the copy number of pLSPYRGAT was more than one and it was 2.4 on average (1.5-3.7 copies).

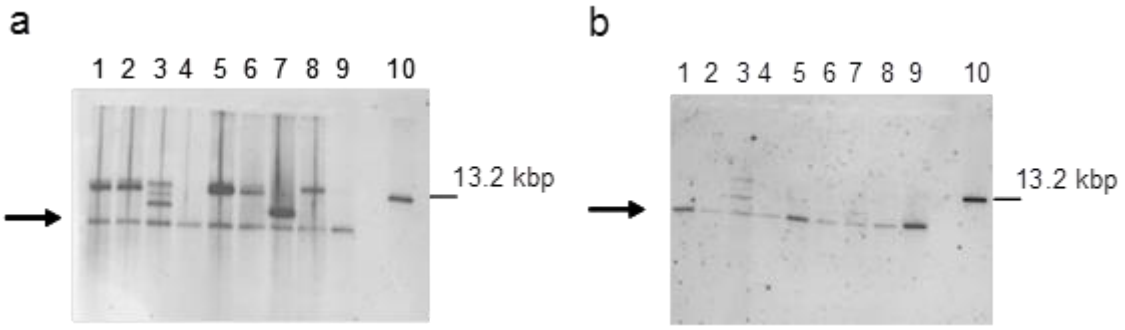

Fig. 3.2. Southern hybridization analysis of transformants harboring an autonomously replicating plasmid. Total DNA was isolated from (a) selective and (b) non-selective culture. A PCR fragment amplified from the *pyrG* ORF was used as the probe (Materials and Methods). Lanes 1 to 8, candidate transformants; lane 9, Ki6 strain (*pyrG*$^{-}$); lane 10, pLSPYRGAT (13.2 kbp). Genomic DNAs were digested with *Bam*HI. The band with an arrow (5.2 kbp) corresponds to the endogenous *pyrG* gene.

3.3.5 Construction of the *ku80*-knockout strain

To enhance the frequency of homologous recombination in the host strain, we disrupted the *ku80* gene in *Lecanicillium* sp. Ki6 by introducing a point mutation (Fig. 3.3a.). Degenerated primer sets designed from the conserved region of fungal Ku80 could amplify a 395 bp-fragment which showed high similarity (80%) to *mus-52* (AB177395) of *Neurospora crassa* (Ninomiya et al. 2004), suggesting that the *Lecanicillium* sp. HF627 also possesses a *ku80* homolog. By screening the partial genomic library of *Lecanicillium* sp. HF627 using primers matching the obtained

PCR-fragment, the entire *ku80* was obtained on a 4,782 kbp-*Eco*RI fragment in which the 2,409 bp-*ku80* ORF [KF147803, 658 amino acid residues, 5 introns, 87% similarity to *mus-52*] together with 1,550 kbp-5' region and 823 kbp-3' region were located.

With the intact *ku80* gene in hand, we constructed the *ku80*-disruption plasmid pKU80MUT, in which a point mutation was introduced to create a stop codon at 221st Lys (Fig. 3.3a), and transformed it into Ki6 (*pyrG*$^{-}$). Twenty-four transformants were analyzed by colony PCR detecting integration of pKU80MUT at correct locus, which resulted in the selection of five positive strains, and they were subjected to Southern hybridization using the *ku80* gene as a probe. Two signals of the expected size (5.0 kbp and 6.0 kbp) were detected from all 5 strains, indicating that the disruption plasmid was integrated by single crossover at the *ku80* locus (Fig. 3.3b). To facilitate the intra-molecular recombination between the intact *ku80* gene and the mutated *ku80* gene, by which the *pyrG* marker gene will be lost, the conidia of the first crossover transformants were spread onto CD^{+} medium containing 5-FOA and uridine. The emerged colonies were further screened for uridine auxotrophy to confirm the loss of *pyrG* by the second crossover. The genotype of the *ku80* deficient strains was analyzed by PCR using the primers, one of which could anneal only to the mutated *ku80*, followed by Southern hybridization using *ku80* as the probe. In the Southern hybridization, a single band was observed at the same position as in the wild-type or *pyrG*$^{-}$ strains, indicating that vector DNA was removed from the chromosome (Fig.

3.3c). Nucleotide substitution on *ku80* was verified by sequencing. The constructed strain was referred to as the Ki50c (*pyrG*$^{-}$ *ku80*$^{-}$) strain and was used for further study.

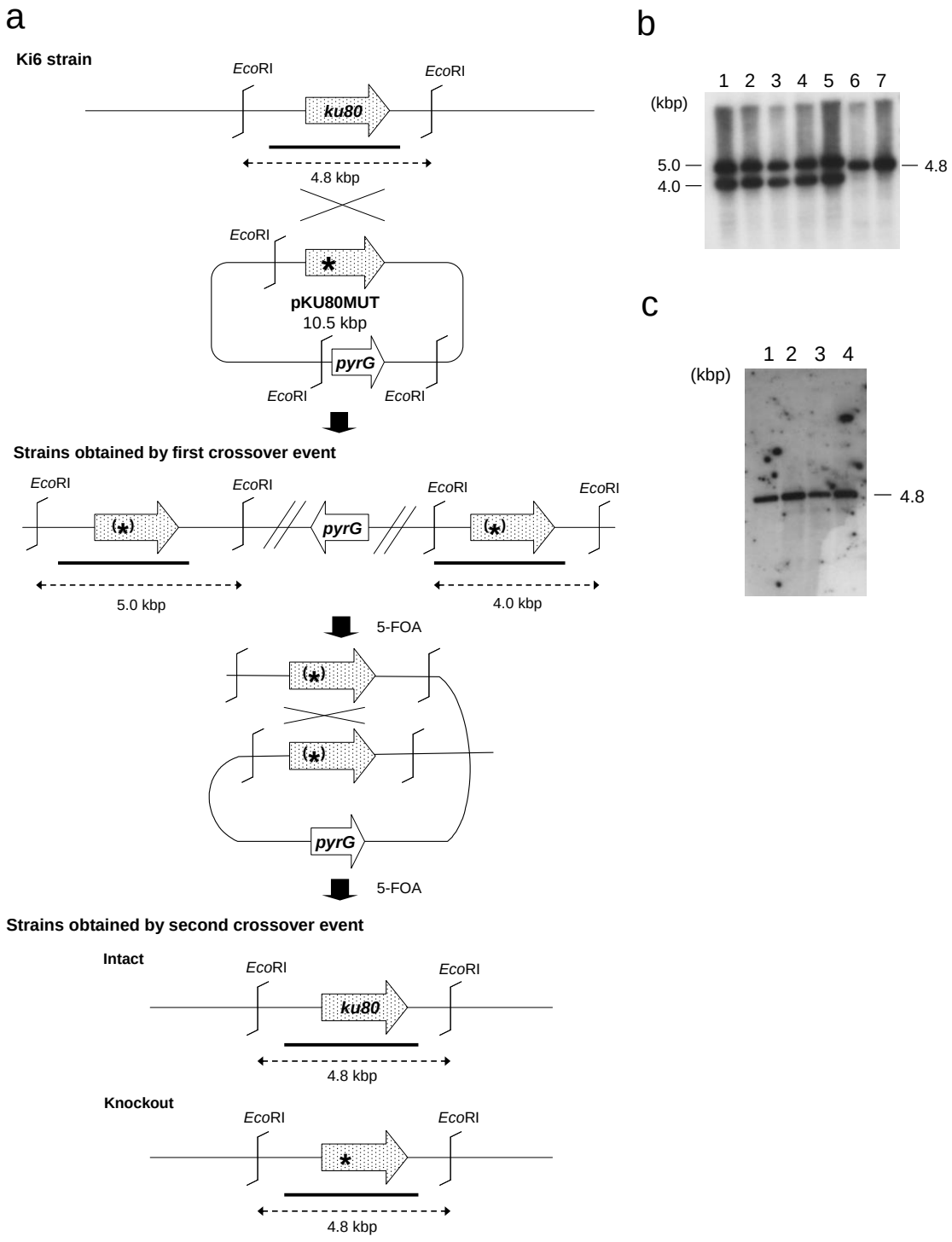

Fig. 3.3 *ku80* knock-out. (a) Schematic strategy to knock out the *ku80* gene. The asterisk indicates a nucleotide substitution from AAG to TAG. pLSPYRG harboring mutated *ku80* (pKU80MUT, 10.5 kbp) was introduced at the *ku80* locus by homologous recombination. The resulting transformant possesses the *pyrG* gene flanked by two copies of the *ku80* gene (*), one intact and another mutated. Intra-molecular recombination between the two *ku80* genes causes the loss of vector DNA from the chromosome, resulting in either a *ku80* knock-out or a revertant containing the intact *ku80*. (b) and (c) Southern hybridization analysis on the crossover strains using *Eco*RI-digested genomic DNA with the *ku80* probe (thick bar in Fig. 3.3a; Materials and Methods). (b) Lanes 1 to 5, candidates for the first crossover strains; lane 6, HF627 strain (wild-type); lane 7, Ki6 (*pyrG*$^{-}$). (c) Lanes 1 and 2, candidates for the second crossover *ku80*$^{-}$ strains; lane 3, HF627 strain (wild-type); lane 4, Ki6 strain (*pyrG*$^{-}$).

3.3.6 Construction of the *pyrG* deletion strain

To further enhance the frequency of homologous recombination at the targeted site, rather than between the *pyrG* locus on the chromosome and the *pyrG* marker on the plasmid, the whole *pyrG* ORF with surrounding locus in the *ku80*$^{-}$ strain was deleted by a similar method as used for constructing the *ku80*$^{-}$ strain (Fig. 3.4; see the Materials and Methods for details of the construction and verification), using crossover between the 0.4 kbp-3' region of *pyrG* and the identical region artificially inserted at the *pyrG* 5'-locus. After transforming the Ki50c (*pyrG*$^{-}$ *ku80*$^{-}$) strain with linearized pPYRGDEL (Fig. 3.4a), the desired strains containing the identical sequence in both the 5'- and 3'-flanking regions of *pyrG* were selected by PCR, and then verified by Southern hybridization. Conidia of the desired strains were grown on the medium containing 5-FOA to facilitate the crossover between the two identical sequences flanking *pyrG* (Fig. 3.4b). The presence of a 3.3 kbp-band in the uridine auxotrophs instead of two bands (4.4 and 2.1 kbp) in the parental strains (Fig. 3.4c) demonstrated that the endogeneous *pyrG* was successfully deleted by intra-molecular recombination. This strain was named Ki2p (*ΔpyrG ku80*$^{-}$) and was used for further gene targeting study.

a

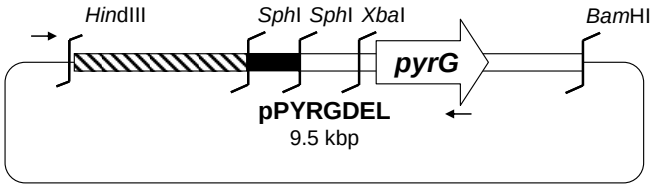
HindIII
SphI SphI XbaI
BamHI
pyrG
pPYRGDEL
9.5 kbp

c

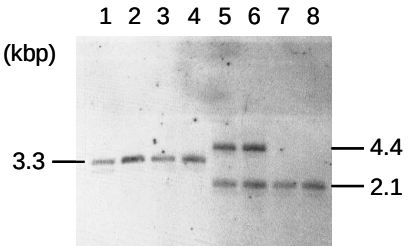
1 2 3 4 5 6 7 8
(kbp)
3.3
4.4
2.1

b

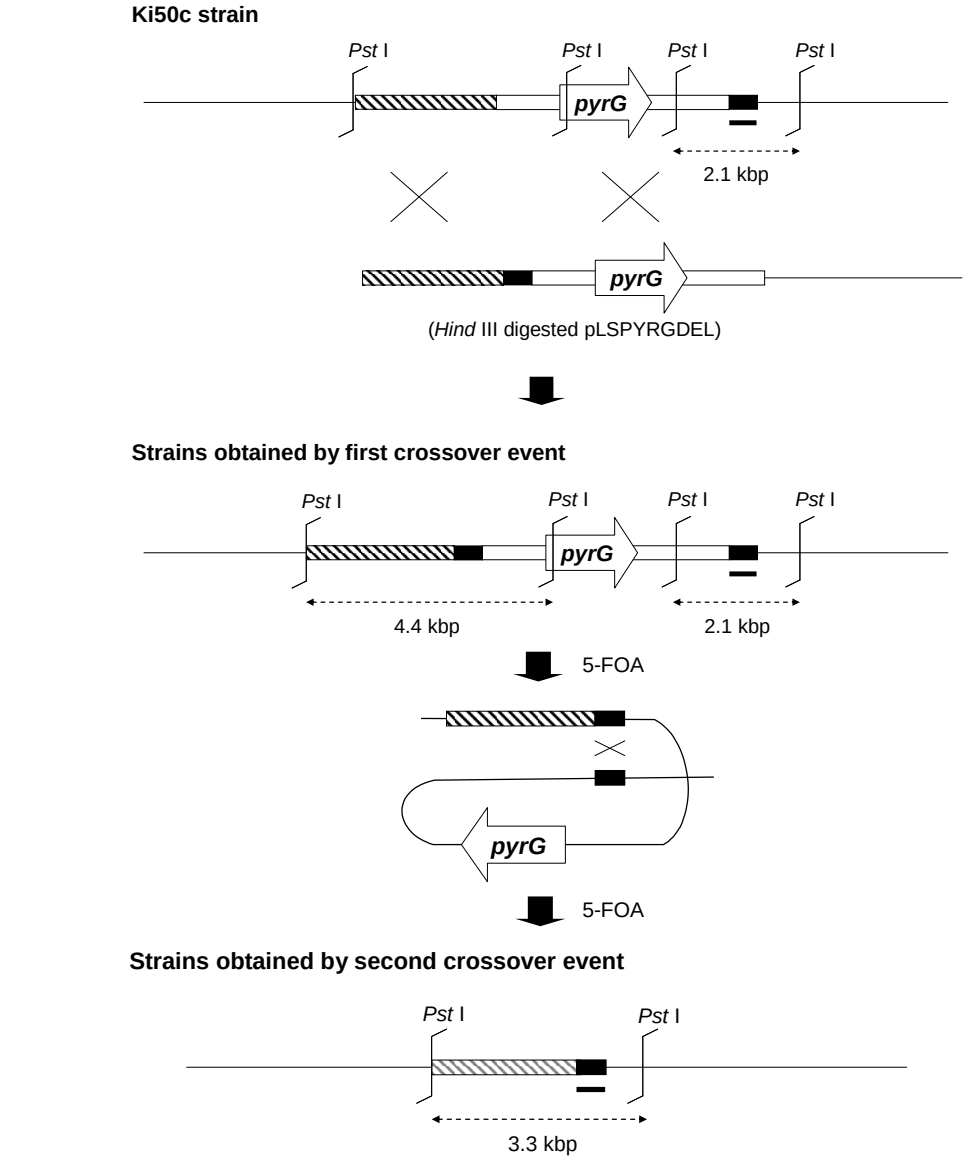
Ki50c strain
Pst I
Pst I
Pst I
Pst I
pyrG
2.1 kbp
pyrG
(Hind III digested pLSPYRGDEL)
Strains obtained by first crossover event
Pst I
Pst I
Pst I
Pst I
pyrG
4.4 kbp
2.1 kbp
5-FOA
pyrG
5-FOA
Strains obtained by second crossover event
Pst I
Pst I
3.3 kbp

Fig. 3.4 Deletion of the *pyrG* locus from the Ki50c strain.

(a) pPYRGDEL (see Materials and Methods for details of the construction). A white box including *pyrG* indicates the initially obtained *Bam*HI/*Sph*I genomic fragment. A hatched box indicates the additionally extended upstream region of *pyrG*. A black box indicates the PCR-amplified 0.4 kbp fragment of *pyrG* downstream inserted at *Sph*I site. Arrows indicate the positions of the primers used to amplify the disruption cassette for transformation.

(b) Schematic strategy to delete endogeneous *pyrG*. A linearized fragment from pPYRGDEL prepared either by *Hin*dIII-digestion or PCR amplification (only the *Hin*dIII fragment is shown in the picture as a representative example) was transformed, and after two rounds of homologous recombination, strain Ki2p (*ΔpyrG ku80*$^{-}$) lacking the entire *pyrG* gene was obtained.

(c) Southern hybridization analysis against *Pst*I-digested genomic DNA to confirm the *pyrG* deletion. Probe, thick bar in Fig. 4.4b. Lanes 1 to 4, second crossover strains as the *pyrG*-deletion mutant; lanes 5 and 6, first crossover strains; lane 7, HF627 (wild-type); lane 8, Ki50c (*pyrG*$^{-}$ *ku80*$^{-}$).

3.3.7 Efficiency of homologous recombination in strain Ki2p (*ΔpyrG ku80*$^{-}$)

To evaluate the efficiency of homologous recombination in the *ku80*$^{-}$ strain of *Lecanicillium*, *trp1* and *his3* (participating in Trp and His biosynthesis, respectively) were chosen as the targets for gene disruption (Table 3.2 and 3.3). When the 1.5 kbp-regions were used for homologous recombination to disrupt *trp1*, the frequencies of Trp auxotrophy from the Ki6 (*pyrG*$^{-}$) parental strains, Ki50c (*pyrG*$^{-}$ *ku80*$^{-}$) and Ki2p (*ΔpyrG ku80*$^{-}$), were 19.6%, 33.3% and 62.5% of all uridine prototrophic strains, indicating that the targeting efficiency increased 3.2-fold. Likewise, the *his3* gene was efficiently disrupted at 62.5% of targeting efficiency in Ki2p, which was 5 times higher than that in Ki6 (12.5%).

Table 3.2. Result of *trp1* targeting experiment

Host strain	Batch	Number of transformants		Frequency of *trp1* disruption (%)
		Total	Trp$^-$ strain	
pyrG$^-$	1st	27	6	22.2
	2nd	19	3	15.8
	Total	46	9	19.6
pyrG$^-$ *ku80*$^-$	1st	15	5	33.3
ΔpyrG ku80$^-$	1st	3	2	66.7
	2nd	12	10	83.3
	3rd	9	3	33.3
	Total	24	15	62.5

Table 3.3. Result of *his3* targeting experiment.

Host strain	Batch	Number of transformants		Frequency of *his3* disruption (%)
		Total	His$^-$ strain	
pyrG$^-$	1st	8	1	12.5
ΔpyrG ku80$^-$	1st	16	10	62.5

3.4 Discussion

In filamentous fungi, exogenous DNA is integrated randomly into the genome by a NHEJ pathway (Bird et al. 1997). The ectopic integration of vector DNA makes the overexpression or complementation experiments very labor-intensive (Shimizu et al. 2012). The expression level of the genes introduced into the fungal chromosome shows high variability that is dependent on the integrated locus (Li et al. 2013), because its expression is controlled by the epigenetic regulation. During the expression experiments, screenings are required to obtain clones which show the proper phenotype. To overcome these problems among filamentous fungi, several significant techniques have been developed. An autonomously replicating plasmid harboring an autonomous replication region (AMA1 sequence) from *A. nidulans* has been applied for overexpression in mainly Eurotiomycetes such as *Aspergillus, Penicillium* and *Monascus* (Fierro et al. 1996; Gems et al. 1991; Shimizu et al. 2006$_b$). This type of vector showed high efficiency of transformation as well as a relatively constant expression of the introduced gene, because the exogenous gene on this vector was not incorporated into the genome, which make the introduced gene expressed independently from the epigenetic regulation. We applied an autonomously replicating vector to our constructed transformation system. pLSPYRGAT successfully restored the uridine auxotrophy of the host strain. Southern hybridization revealed that the introduced plasmid replicated autonomously in the cells grown under a selective culture condition, while all transformants replicated

under nonselective conditions lost the vector (Fig. 3.2). This instability of the vector using AMA1 sequence as the replicating origin is same as the case of *M. anisopliae* (Singkaravanit et al., personal communication). Judging from the band intensity in Southern hybridization, although the copy number of the vector was variable, more than one copy (average 2.4) was observed under the selective conditions (Fig. 3.2). This vector pLSPYRGAT showed significantly higher transformation efficiency (16.7-fold) than that by the integrating vector, although the increase in frequency was moderate compared to the cases of *A. nidulans* (250-fold), *P. chrysogenum* (310-fold), *M. purpureus* (5-fold), *Gibberella fujikuroi* (2-fold) and *Rosellinia necatorix* (5-fold) (Brückner et al. 1992; Fierro et al. 1996; Gems et al. 1991; Shimizu et al. 2006$_b$, 2012). Taking these facts together, we expect that this autonomously replicating vector system will be utilized for heterologous overexpression and functional complementation.

Another significant issue is that NHEJ-dependent ectopic integration of vector DNA causes low frequency of homologous recombination, which hampers gene knock-out studies in filamentous fungi. To improve the frequency of homologous recombination, the component involved in the initial part of NHEJ (Ku70 and Ku80) has been deleted, resulting in 70-100% homologous recombination frequency (Chan et al. 2010; Ninomiya et al. 2004; Takahashi et al. 2006; Villalba et al. 2008). Despite these reports, knock out of the *ku80* gene in *Lecanicillium* sp Ki6. did not substantially increase the targeting efficiency (the efficiency remained at 62.5% at both the *trp1* locus and *his3*

locus), although the homologous arms used were relatively long (1,500 bp). This frequency is rather lower than those in other filamentous fungi, such as *N. crassa* (93%, *Δku80*, 500 bp homologous arms), *A. sojae* (71%, *Δku70*, 500 bp), *Coprinopsis cinerea* (82%, *Δku70*, 500 bp), *Sordaria macrospora* (100%, *Δku70*, 1,000bp), *A. fumigatus* (80%, *Δku80*, 1.5 kbp), *Hypocrea jecorina* (96%, *Δku70*, 1,000bp) and *A. nidulans* (89%, *Δku70*, 500 bp) (da Silva Ferreira et al. 2006; Guangtao et al. 2009; Nakazawa et al. 2011; Nayak et al. 2006; Ninomiya et al. 2004; Pöggeler and Kück 2006; Takahashi et al. 2006). This might be attributed to the existence of a KU-independent NHEJ pathway, as proposed in *N. crassa* (*mus-11*) and *S. cerevisiae* (*RAD52*) (Ishibashi et al. 2006; Yu and Gabriel 2003). A BLAST search with the sequence of Mus-11 against the draft genome sequence of strain HF627 detected a highly similar gene (74%) to *mus-11*, suggesting that the gene product might play an alternative role in the NHEJ pathway in *Lecancillium* spp. Consistent with the hypothesis that KU-independent NHEJ pathway exists in *Lecanicillium*, ectopic integration of *trp1* disruption vector was confirmed in Trp prototrophic strains by Southern hybridization experiment (data not shown). Although inactivation of the above-mentioned *mus-11* ortholog or *lig4* gene encoding DNA ligase IV might be required to achieve a higher gene targeting efficiency, the drastic increase of the targeting efficiency achieved with the strain Ki2p should facilitate reverse genetic studies in *Lecanicillium*.

3.5 Summary

In this chapter, a transformation system of *Lecanicillium* sp. HF627 was constructed by creating a uridine auxotrophic mutant strain as the host and using an endogenous *pyrG* gene as a marker. In the system, an autonomously replicating plasmid as well as the integrating vector were available. To make this system applicable for gene targeting study, *ku80* homolog which is a component of nonhomologous end-joining (NHEJ) pathway was knocked-out. Furthermore, *pyrG* locus was deleted to eliminate the competitive inhibition against the homologous recombination at a target locus, resulting in enhanced frequency of homologous recombination. Thus, the system which enables functional analysis of genes by both overexpression and knock-out experiments in *Lecanicillium* sp. HF627 strain was constructed.

Chapter 4

Identification of a gene cluster responsible for the biosynthesis of cyclic lipopeptide verlamelin

4.1 Introduction

Structurally verlamelin is a cyclic hexadepsipeptide, and is bridged by ester bonding between a hydroxy group on a fatty acid moiety and a carboxyl group on the terminal Val of amide-bonded tetradecanoyl-hexapeptide (Thr-Ala-Pro-Gln-Tyr-Val). Most cyclic depsipeptides of fungal origin are synthesized by non-ribosomal peptide synthethases (NRPS) and composed of amino acids, but some contain fatty acid moieties. However, the majority of these fatty acids are derived from common amino acids, such as α-hydroxyisocaproic acid, which is converted from Leu (Wang et al. 2012), and only a few of them (e.g., emericellamide or FR901469) contain linear branched-chain fatty acids, which may be derived from fatty acid synthase (FAS) or polyketide synthase (PKS) (Chiang et al. 2008; Fujie et al. 2000). As for genetic studies on the biosynthesis of peptides in filamentous fungi, many of these reports have focused on genes encoding NRPS, which is a multifunctional enzyme composed of modules corresponding to the order of amino acids in the structure of cyclic peptides (Marahiel et al. 1997). Although a number of biosynthetic clusters have been clarified, there have been only a few detailed biosyntheses of cyclic peptides which contain a long/middle-chain fatty acid moiety, such as apicidin or echinocandin (Cacho et al. 2012; Jin et al. 2010).

In this chapter, NRPS gene responsible for the biosynthesis of verlamelins, which

contain 5-hydroxytetradecanoic acid moiety synthesized either by FAS or PKS was characterized. Further analysis of genes flanking the NRPS gene together with gene disruptions revealed the presence of a verlamelin biosynthetic-gene-cluster, and the probable biosynthetic pathway/mechanism of verlamelin was described based on the cluster analysis.

4.2 Materials and Methods

4.2.1 Strains and media

Lecanicillium sp. HF627, isolated from a chillie thrips cadaver, was used as a wild-type strain. Ki6 (*pyrG*$^{-}$ *ku80*$^{-}$) and Ki2p (*ΔpyrG ku80*$^{-}$) strains created from HF627 (chapter 3) were used as the parental strains for the functional analysis of verlamelin biosynthetic genes. *Escherichia coli* DH5α was used for the construction and propagation of plasmids. YES medium (8% sucrose, 4% yeast extract) and SMY medium (4% maltose, 1% yeast extract, 1% peptone) were used as production media of verlamelin. Conidia were collected from strains grown on potato dextrose agar (PDA) (Difco), supplemented with 10 mM of uridine as required. CD^{+} medium was prepared by the addition of 0.2% of $(NH_4)_2SO_4$ to Czapek-Dox (CD) medium (Oxoid, Hampshire UK) (with 1.5% of agar for plate), and was used as a limited medium of uridine. CD^{+} medium supplemented with 0.8 M KCl was used for transformation of Ki6 and Ki2p.

4.2.2 Plasmids

pLSPYRG containing *pyrG* from HF627 was constructed on pUC19 as described in chapter 3. For constructing disruption vectors, a 1.2 kbp-region downstream of *pyrG* was amplified by PCR with a primer pair (Table 4.1, pyrgfoa1-pyrgfoa2), and was cloned into the *Sph*I/*Hin*dIII sites of pLSPYRG, yielding pLSPYRG1200R, with which *pyrG* with the promoter region can be eliminated from the transformants via homologous recombination.

4.2.3 Vector insertion into a locus of the NRPS gene

A 1.6 kbp-fragment of the NRPS gene was amplified by PCR using PrimeSTAR® HS DNA Polymerase (Takara) with a primer pairs (nrpsDdis1-nrpsDdis2). The PCR fragment was cloned into the *Xho*I/*Sac*I site of pLSPYRG, yielding the NRPS-targeting vector (pDISNRPSD).

Strain Ki6 was transformed as described in chapter 3 using the constructed vector (pDISNRPSD). Emerged colonies on the selection plates were screened by PCR using an FTA® classic card (Whatman®) with a primer pair (nrpsDdischeck-M13fw). The genotypes of the candidate strains were further analyzed by Southern hybridization with a probe prepared by PCR (nrpsD1-nrpsD2) against *Eco*RI-digested genomic DNA.

4.2.4 Transcriptional analysis of *vlmS*-proximal genes

The wild-type strain was statically cultivated in 20 ml of YES and SMY media in 100-ml Erlenmeyer flasks at 25°C for 5 days. Total RNA was isolated from a mycelial mat using an RNeasy plant minikit (Qiagen), and treated with DNase I (Takara). The cDNA was synthesized using Superscript III RNaseH$^-$ (Invitrogen) with random primers (Invitrogen) according to the manufacturer's instruction. RT-PCR was performed using GoTaq green master mix (Promega KK) with primer pairs (orfA1-orfA2, orfB1-orfB2, orfC1-orfC2, orfD1-orfD2, orfE1-orfE2, orfF1-orfF2, orfG1-orfG2, orfH1-orfH2, orfI1-orfI2, orfJ1-orfJ2, act1-act2, nrpsD1-nrpsD2, Table 4.1) under the following conditions: 94°C for 5 min, and 30 cycles of 94°C for 30 sec, 55°C for 30 sec, and 72°C for 30 sec, followed by a final elongation step at 72°C for 7 min.

4.2.5 Disruption of *vlmS*-proximal genes

Each of five genes (*orf-a, orf-b, orf-c, orf-d* and *orf-g*, clustering around *vlmS*) was disrupted by targeted replacement with *pyrG*. Each of the 5'-upstream fragments was amplified by PCR using PrimeSTAR® HS DNA Polymerase (Takara) or TaKaRa Ex Taq® (Takara) with primer pairs (orfAdisN1-orfAdisN2, orfBdisN1-orfBdisN2, orfCdisN1-orfCdisN2, orfDdisN1-orfDdisN2 and orfGdisN1-orfGdisN2, respectively), yielding 1.6, 1.5, 1.5, 1.6 and 1.4 kbp fragments, respectively. Similarly, 3'-downstream

fragments were also PCR-amplified with primer pairs (orfAdisC1-orfAdisC2, orfBdisC1-orfBdisC2, orfCdisC1-orfCdisC2, orfDdisC1-orfDdisC2 and orfGdisC1-orfGdisC2, respectively), yielding 1.5, 1.5, 1.5, 1.5 and 1.8 kbp fragments, respectively. The cognate 5'- and 3'-fragments were cloned on pLSPYRG (for *orf-b* and *orf-g*) or pLSPYRG1200R (for *orf-a*, *orf-c* and *orf-d*), making the *pyrG* gene flanked by the 5'- and 3'-fragments. The disruption vector was linearized by digestion with *Hin*dIII (for the *orf-a, orf-b*, and *orf-d* disruption vectors) or *Sac*I (for the *orf-c* and *orf-g* disruption vectors) prior to transformation. Transformation of Ki2p was carried out as described in chapter 3. Emerged colonies on the selection plates were screened by PCR using an FTA® classic card (Whatman®) with primer pairs (orfA2-pprv, orfF1-pprv, nrpsDup-pp1200fw, orfB1-pp1200fw and orfC1-pp1200fw, respectively). The genotypes of candidate strains were confirmed by Southern hybridization using probes prepared by PCR with primer pairs (orfB1-orfB2 for *orf-a* and *orf-b*; orfC1-orfC2 for *orf-c* and *orf-d*; and orfH1-orfH2 for *orf-g*).

4.2.6 Verlamelin production in disruptants

The production profile of low-Mr compounds was analyzed by HPLC. Cultures of the wild-type and transformants were prepared by static cultivation with 20 ml of YES medium in 100-ml Erlenmeyer flasks at 25°C for 5, 10 and 15 days. Whole cultures including the mycelial mat were extracted with *n*-butanol (10 ml) by mild shaking for

one hour, followed by vigorous shaking for one minute. The *n*-butanol layer was collected after centrifugation (3000 rpm, 10 min) and evaporated *in vacuo*, and the residue was dissolved in methanol or DMSO (for the preparation of further concentrated samples) for HPLC analysis using an Imtakt Cadenza CD-C18 (Ø4.6 x 75 mm) column with a linear gradient of CH_3CN from 15% to 85% in 0.1% formic acid aqueous solution, at a flow rate of 1.2 ml/min (3 min at 15%, 3 min from 15% to 40%, 6 min at 40%, 7 min from 40% to 45%, 3 min from 45% to 85%, 7 min at 85%, 3 min from 85% to 15%).

4.2.7 Feeding experiment of 5-hydroxytetradecanoic acid

5-Hydroxytetradecanoic acid was obtained by cleaving the lactone ring of δ-tetradecanolactone (TCI, Japan) by the following procedures. δ-tetradecanolactone (50 mg) was dissolved in 1M NaOH in methanol/water (4/1) and stirred overnight at room temperature. After neutralization with 1M HCl, the reactant was extracted with *n*-hexane and concentrated in vacuo, followed by purification with silica gel chromatography using a hexane-AcOEt solvent system (4/1, 2/1, 1/1, 0/1). Fractions containing 5-hydroxytetradecanoic acid (Rf value 0.17, versus 0.5 for δ-tetradecanolactone) on silica gel TLC (Hexane/AcOEt; 2/1) were pooled and dried in vacuo, yielding 5-hydroxytetradecanoic acid (10 mg, m/z 245 by CI^+MS). Disruptants of *vlmA* and *vlmB* were grown statically in YES liquid medium at 25°C. After 4 days of

cultivation, 5-hydroxytetradecanoic acid was added at a final concentration of 0.2, 0.4, or 0.8 mM, and the culture was harvested after an additional 6 days of cultivation for verlamelin analysis.

Name	Sequence (5'-3')
pyrgfoa1	GGGAAGCTTACTAGTAGATCTGGAAGTCATTGAAATC
pyrgfoa2	TAGCATGCATATCCACAAGCTGGTCAA
coa1	GGAATTCTAGASNCCNKCNTGGGTNCC
coa4	GGAATTCTAGACCNGWNGTNCCRCTNGT
A0S1	GGAATTCTAGATWYACNWSNGGNTC
A2	GGAATTCTAGAYTCNSHNGGNCCRTA
T1S1	GGAATTCTAGAHNGARTCNCCNCC
A2C	GGAATTCTAGATAYGGNCCNDSNGA
A3	GGAATTCTAGARTCNCCNGTNYKRTA
nrpsDdis1	GGGCTCGAGATGGAAAAGTCCAAACT
nrpsDdis2	GGGAGCTCGAAAAAGTTGGCAGAAT
nrpsDdischeck	CCATGGTCGGTATGTGT
M13fw	GTAAAACGACGGCCAGT
nrpsD1	CTGCTCTGAACATAGGA
nrpsD2	TTGAGCTCGGCAACAAA
orfA1	GCATACGCGGATTCAGA
orfA2	CGATCCCATATCCGAGT
orfB1	GCTGCCAATCAGGCAAT
orfB2	CCTTGGATGGGATGATG
orfC1	CTGTCGGATCTTTAGCA
orfC2	GAATCAGGCCAACATCT
orfD1	TTGCGCCATTCTCCACT
orfD2	CACCGTCGTGGACAATA
orfE1	TCCAACTTGGGCTGGTA
orfE2	TGAGACCGACTTCGGTA
orfF1	AGCCCTTGGACCTTCAT
orfF2	GCAAGACTCGCTGTAGA
orfG1	GCTGACTGCCTCATTCT
orfG2	GGATTCAGGCCTTGACT
orfH1	CAGGTGGTCCAGGTATT
orfH2	AGGCAGAGTCCATGTTG
orfI1	GTAGGTGGATGGAGTCA
orfI2	CTGGCAACTCTTGCTGT
orfJ1	AGCGGCAAGGTCTACAA
orfJ2	TCAGCGGCACAGATCAT
act1	CCGAATTCCACCGATCCAGACAGAGTACTTTCGC ACTTTCGC
act2	CCGAATTCGACATCAAGGAGAAGCTCTGCTACGTCTGCTACGTCACTTTCGC

orfAdisN1	CTGGTACCGTATGCCACCAGGACA
orfAdisN2	CTGAGCTCGTACGAAGCGGCCTCAA
orfBdisN1	GTGAGCTCACCAACTGTGAGAGGAA
orfBdisN2	GGGGATCCTCTAGGCCAGTATGCAC
orfCdisN1	GTCAAGCTTGCTTGAACATGATGGCT
orfCdisN2	CTGAGATCTACGGGTATTGATCTCGT
orfDdisN1	GTCAAGCTTCGAATGAGAAACGATGA
orfDdisN2	GTTAGATCTCTTTAAGTTGCTGTGCT
orfGdisN1	CCGCATGCAGCAACATTGGTCCTGT
orfGdisN2	CCTAAGCTTACAATGAGTGCAGGTGA
orfAdisC1	AGCAAGCTTGATTGCTTGGTGGTTGA
orfAdisC2	GGTAGATCTGCAGATCGCATTGAGAC
orfBdisC1	CAGCATGCTTGAACATGATGGCTT
orfBdisC2	CAAAAGCTTGAATTGGTTGTTCCTCT
orfCdisC1	AAGGTACCTGGCGACAGAATGGAAC
orfCdisC2	CCGAGCTCGACTTGATGGCCCTAA
orfDdisC1	TGGGTACCAGTTACCAAACTCCAGA
orfDdisC2	TTGAGCTCTAATTACAGCGCTGTT
orfGdisC1	GAGAGCTCAATTGGACGACGTCAA
orfGdisC2	GTGGATCCTGCGATTACCAAGTGTC
pprv	AGGGAAATCCTCCTCGA
nrpsDup	AAATTAGTTGATGAGCAC
pp1200fw	TCAATGACTTCCAGATC

Table 4.1. Oligonucleotide used in this study

4.3 Results

4.3.1 Identification of an NRPS gene responsible for verlamelin biosynthesis

The fact that the peptidyl moiety of verlamelin A and B was composed of D-amino acids as well as L–amino acids indicates that this moiety is probably synthesized by a nonribosomal peptide synthetase (NRPS). Based on the conserved sequences of the adenylation domains and peptidyl carrier protein domains in NRPSs (Marahiel et al. 1997), PCR primers (Table 4.1) were designed, and RT-PCR was conducted with RNA isolated from the *Lecanicillium* mycelia grown under verlamelin production conditions, resulting in five different PCR fragments encoding putative adenylation domains of NRPS. To identify the NRPS gene responsible for the verlamelin biosynthesis, each adenylation domain was disrupted by inserting a *pyrG* gene through homologous recombination. HPLC analysis of low-MW metabolites from each transformant demonstrated that disruption of an adenylation domain from one of the PCR fragments caused a complete loss of verlamelin production (Fig. 4.1A), while disruption of other adenylation domains did not affect the production of verlamelin (data not shown).

Based on the sequence information causing the loss of verlamelin, the whole coding sequence of the NRPS gene was identified in the draft genomic sequence of *Lecanicillium* sp. HF627, and the NRPS gene responsible for the verlamelin biosynthesis was named *vlmS* (AB862312). The *vlmS* gene containing one putative intron (50 n.t., predicted based on the presence of consensus sequence) was 26,762 n.t. encoding an

8,903-amino-acid protein which showed highest similarity (90%) to NRPS from *Fusarium pseudograminearum* (EKJ70673). Domain analysis with Pfam using the deduced amino acid sequence as query detected seven modules composed of seven peptidyl carrier protein domains, six adenylation domains, seven condensation domains and four epimerization domains, while the initial module at the N-terminus lacked the adenylation domain (Fig. 4.2B). One of the epimerization domains in the initial module appeared to be inactive, because the catalytic His residue was substituted to Ala. The number of modules and the presence of epimerization domains in the 2^{nd}, 3^{rd}, and 6^{th} modules matched the structure of the peptidyl moiety of verlamelin A and B.

4.3.2 Biosynthetic genes for verlamelin in the flanking regions of *vlmS*

Because all the genes necessary for the biosynthesis of a particular secondary metabolite are almost always clustered (Brakhage et al. 2011), to identify the remaining genes essential for the verlamelin biosynthesis, both the 5'- and 3'-flanking regions of *vlmS* were analyzed. Sequence analysis and a database search with BLASTX revealed ten flanking genes (Fig. 4.2A and Table 4.2). Transcriptional analysis of the ten genes by RT-PCR using RNA isolated from cells grown under verlamelin production conditions revealed that six genes (*orf-a, orf-b, orf-c, orf-d, orf-g and orf-h*) among the ten were transcribed (Fig. 4.2C), suggesting that *vlmS* and the six genes may constitute the verlamelin biosynthetic gene cluster, although *orf-h* (encoding AAA ATPase) should be

eliminated from the putative cluster, considering that ATPase seems unlikely to be involved in the verlamelin biosynthesis.

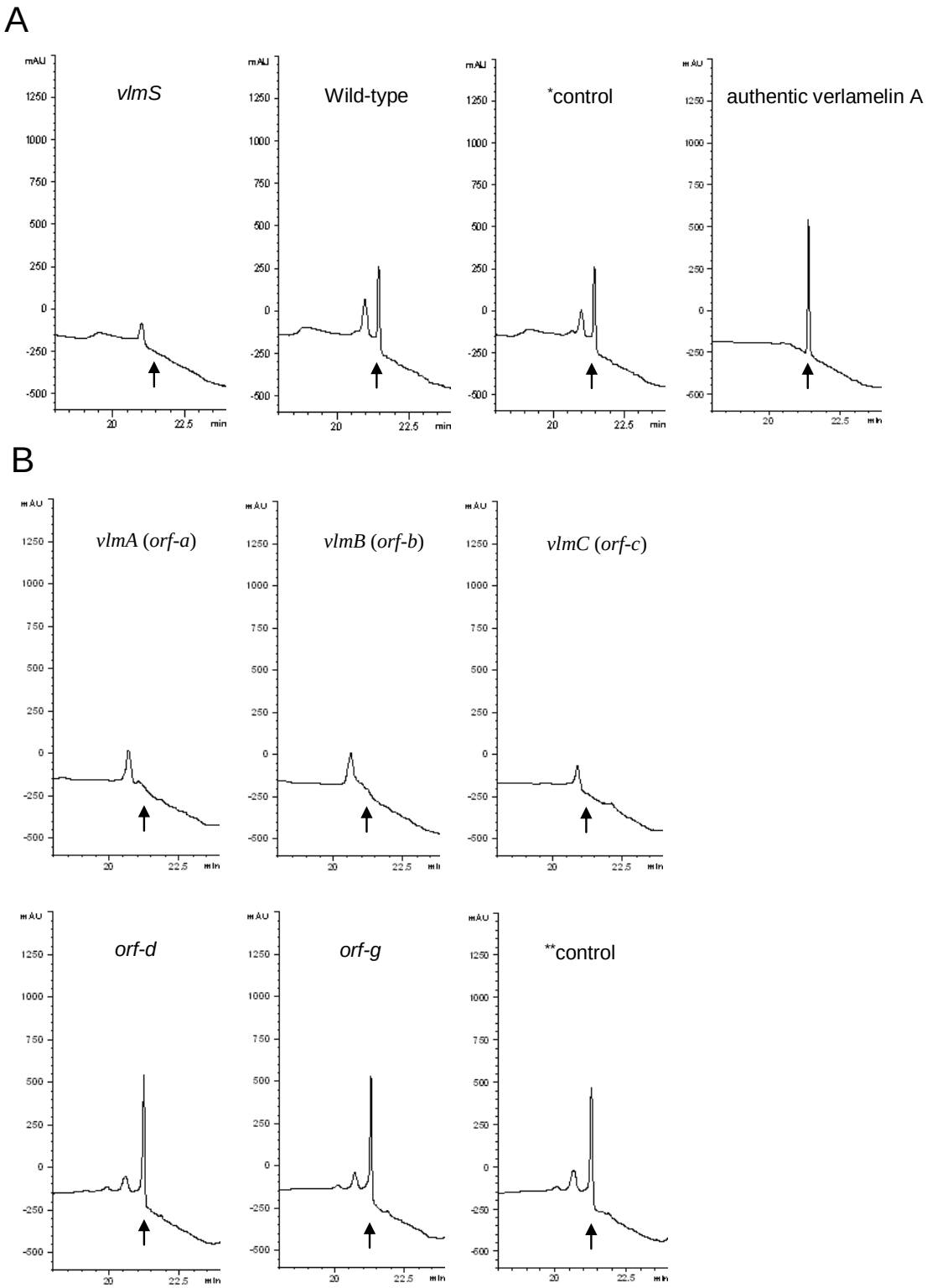

Fig. 4.1.. HPLC analysis of the *vlmS* disruptant (A) and disruptants of *orf-a*, *orf-b*, *orf-c*, *orf-d* and *orf-g* (B). Control strains were obtained by non-targeted integration of *pLSPYRG to the ki6 strain (chapter 3) and ** and non-targeted integration of the *orf-c* disruption vector to the ki2p strain, respectively. The chromatograms were recorded with detection at 210 nm. Arrows indicate the elution position of verlamelin A (1).

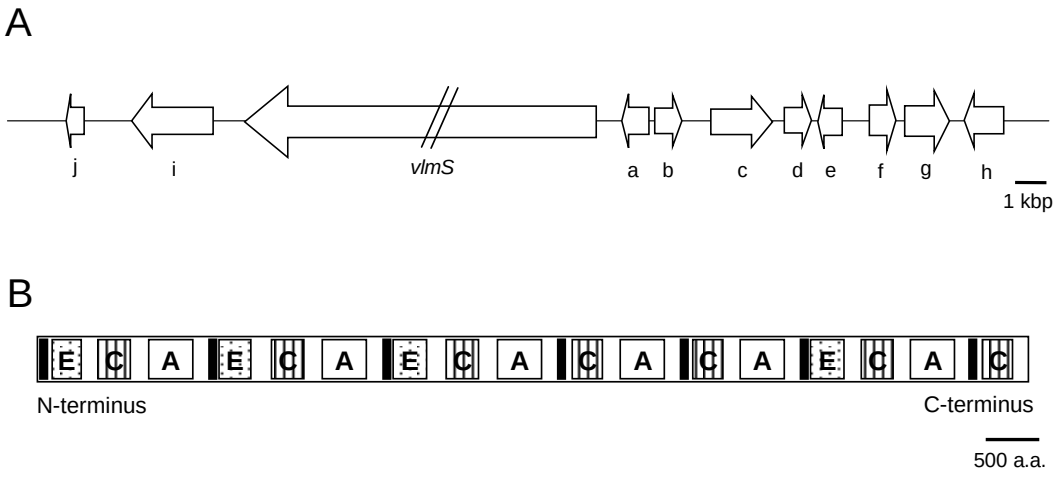

Fig. 4.2. Verlamelin biosynthetic gene cluster. (A) Gene organization around *vlmS*. The direction of the white arrows corresponds to that of the reading frame. (B) Domain structure of VlmS. The white boxes labeled A represent adenylation domains. The striped boxes labeled C represent condensation domains. The dotted boxes labeled E represent epimerization domains. Black boxes represent peptidyl carrier protein domains. (C) RT-PCR analysis of ORFs found in the 50-kbp neighboring region of *vlmS* under the verlamelin-producing conditions [YES medium (upper panel) and SMY medium (lower panel)]. a, *orf-a* (*vlmA*); b, *orf-b* (*vlmB*); c, *orf-c* (*vlmC*); d, *orf-d*; e, *orf-e*; f, *orf-f;* g, *orf-g*; h, *orf-h*; i, *orf-i*; j, *orf-j*; act, actin gene as a positive control; s, *vlmS*. Pictures of gels were taken under UV light after staining with ethidium bromide. No transcription of *orf-e*, *orf-f*, *orf-i* or *orf-j* was detected, although several PCR conditions and different primer sets were tested (data not shown).

Table 4.2. Genes located in and adjacent to the verlamelin biosynthesis gene cluster.

Gene	Size (bp)	Predicted function[a]	Most similar homologue		
			Origin	Accession No.	Identity/Similarity (%)
vlmS (AB862312)	26,762	non-ribosomal peptide synthase	*Fusarium pseudograminearum* CS3096	EKJ70673	59/90
vlmA (AB862313) (*orf-a*)	1,098	fatty acid hydroxylase	*Fusarium oxysporum* f. sp. cubense race 4	EMT72758	46/78
vlmB (AB862314) (*orf-b*)	696	thioesterase	*Epichloe festucae*	AET11897	72/92
vlmC (AB862315) (*orf-c*)	2,045	AMP dependent ligase	*Epichloe festucae*	AET11896	76/94
orf-d	704	glutathione S-transferase	*Metarhizium acridum* CQMa 102	EFY84422	46/74
orf-e	757	MFS transporter	*Penicillium chrysogenum* Wisconsin 54-1255	XP_002558829	34/75
orf-f	1,196	dehydrogenase	*Trichoderma atroviride* IMI 206040	EHK51082	59/89
orf-g	2,203	$Zn(II)_2Cys_6$ transcription factor	*Fusarium pseudograminearum* CS3096	EKJ68669	47/83
orf-h	2,033	AAA ATPase	*Nectria haematococca* mpVI 77-13-4	XP_003050142	53/88
orf-i	2,217	peptidase	*Fusarium oxysporum* f. sp. cubense race 4	EMT67983	47/83
orf-j	756	trypsin	*Cordyceps militaris* CM01	EGX95217	45/85

[a]The functions of genes were predicted based on the conserved domain of putative products.

To further examine which of the five genes are involved in the verlamelin biosynthesis, each of the five genes was disrupted by homologous recombination with *pyrG* insertion as the marker. After confirming the genotype of uridine prototroph by Southern hybridization, the disruptant of each gene was cultivated under verlamelin production conditions, and verlamelin production was analyzed by C18 HPLC (Fig. 4.1B). Verlamelin production was mostly/completely lost by disruption of *orf-a, orf-b* and *orf-c*, but remained intact by disruption of *orf-d* or *orf-g*, demonstrating that only three genes (*orf-a, orf-b, and orf-c*) together with *vlmS* are involved in the verlamelin biosynthesis. Although the productivity of verlamelin was deficient in both the *orf-a* and *orf-c* disruptants, it was slightly retained in the *orf-b* disruptant (less than 5% of that in the wild type). As for the morphology and growth, no significant differences were observed between the disruptants (data not shown).

Based on these results, three genes (*orf-a, orf-b* and *orf-c*) were concluded to be components of the verlamelin biosynthetic pathway and were named *vlmA* (AB862313), *vlmB* (AB862314) and *vlmC* (AB862315), respectively. VlmA showed similarity to proteins belonging to the fatty acid hydroxylase superfamily, including C-5 sterol desaturase *ERG3* (NP_013157, 67% similarity to VlmA) and methylsterol methyl monooxygenase *ERG25* (NP_011574, 63% similarity to VlmA) of *S. cerevisiae*. VlmA contains three histidine-rich motifs (essential for metal binding) that are conserved among other proteins in this family. VlmC was deduced to be AMP-dependent ligase,

which is classified into a group involving acyl-CoA synthetase and the NRPS adenylation domain, both of which catalyze the formation of thioester via activation of carboxylic acid by adenylation (Gulick et al. 2009). The genes with the highest similarity in the fungal secondary metabolism were EasD (XP_660153, 76% similarity to VlmC) and EcdI (AFT91380 76% similarity to VlmC), both of which are fatty acid-activating enzymes in the lipopeptide biosynthesis of emericellamide and echinocandin produced by *A. nidulans* and *Emericella rugulosa* respectively (Cacho et al. 2012; Chiang et al. 2008). As for VlmB, although three proteins belonging to the thioesterase superfamily showed high similarity (AET11897 of *Epichloe festucae*, EGU84193 and ENH63667 of *Fusarium oxysporum*, 83-92%,), no information on their functions, substrates or products was available.

4.2.3 Feeding experiment of 5-hydroxytetradecanoic acid

To identify the gene(s) involved in the supply of 5-hydroxytetradecanoic acid (an immediate precursor for verlamelin biosynthesis), a feeding experiment was conducted on the disruptants of *vlmA* and *vlmB*. The loss/decrease of verlamelin production was complemented both in *vlmA* (7.7%, 9.6% and 23.4% by 0.2, 0.4 and 0.8 mM) and *vlmB* (9.3% and 12.4% by 0.2 and 0.4 mM), while the productivity was much lower than that of the wild-type phenotype (Fig. 4.3). Thus, *vlmA* and *vlmB* were demonstrated to function in 5-hydroxytetradecanoic acid synthesis.

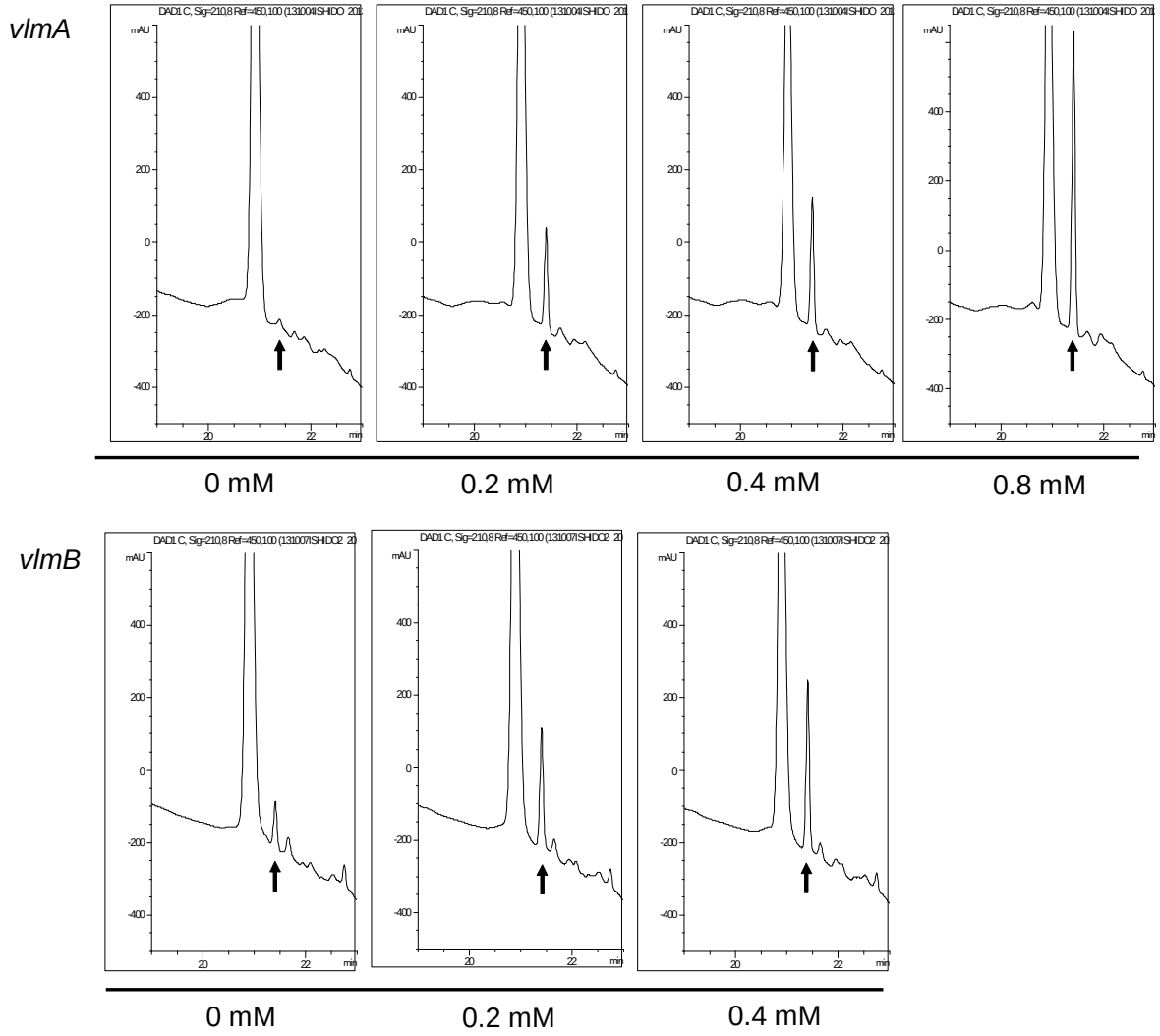

Fig. 4.3. Feeding experiment of 5-hydroxytetradecanoic acid. The chromatograms were recorded with detection at 210 nm. Arrows indicate the elution position of verlamelin A (**1**). Verlamelin A production level in the no-feeding control culture of *vlmB* disruptant was 3.3% of wild-type level. Size of the peak eluted immediate before verlamelin A was much larger than that detected in Fig. 4.1, probably due to the difference of organic solvent used to dissolve (DMSO instead methanol) the culture extracts.

4.4 Discussion

The NRPS gene responsible for the verlamelin biosynthesis was identified and named *vlmS* (AB862312). Analysis with the Conserved Domain Database (CDD) revealed that VlmS is composed of seven modules, among which the initial module at its N-terminus lacks an adenylation domain (Fig. 4.2B). The lack of an adenylation domain in the initial module is same as the cases of EcdA (AFT91378) and EasA (XP_660149), which are NRPSs for biosynthesis of the lipopeptides echinocandin and emericellamide, respectively (Cacho et al. 2012; Chiang et al. 2008). In both cases, the initial module is considered to accept the fatty-acyl intermediate as the starter compound for further peptide elongation, and thus VlmS should be considered to accept a fatty-acyl intermediate with the initial module to further elongate amino acid residues by the downstream modules. In addition, in the last module at its C-terminus, VlmS contains a surplus condensation (C) domain that should be active, based on the presence of the conserved catalytic His residue and the high similarity with other C domains in the database [65-75% to each of seven C domains in EcdA (AFT91378)]. Because a set of domains in the typical domain arrangement, (C domain-A domain-PCP domain), that is necessary for simple elongation of the last amino acid already exists in this module, the surplus C domain seems to have another function, such as cyclization as the last step to form verlamelin, from the analogy that most fungal NRPSs utilize an additional C-terminal thioesterase domain (Gao et al. 2012;

Haynes et al. 2011) to cyclize linearly mature peptides. From the concomitant production of verlamelin A and B, which differ only in the second amino acid residue (D-alloThr or D-Ser), the substrate specificity of the adenylation domain in the 2nd module appears to be relaxed, accepting not only Thr but Ser as a substrate, although Thr is the more preferred substrate.

Regarding the gene cluster, four genes [*vlmS* (AB862312), *vlmA* (AB862313), *vlmB* (AB862314) and *vlmC* (AB862315)] were identified as the cluster components responsible for the verlamelin biosynthesis. Among the ten genes existing in the vicinity of *vlmS*, five genes were initially selected from their coincidental transcriptions under the verlamelin production conditions and their putative functions in the biosynthesis of secondary metabolites (Fig. 4.2 and Table 4.2), but two (*orf-d*, and *orf-g*) were eliminated based on the normal verlamelin production in the corresponding disruptants. It was unexpected that *orf-g* is not involved because it encodes a member of the $Zn(II)_2Cys_6$-type transcriptional regulators, which are commonly present in fungal secondary metabolic gene clusters (Baba et al. 2006; Shimizu et al. 2007; Yu et al. 1996), where they function to ascertain the synchronized expression of necessary structure genes. Because no other regulatory genes are present in the vicinity of *vlmS*, but direct/inverted repeats of GTAC-N_{1-3}-GTA(C/G) are present in the 150-300 bp region upstream of only the four verlamelin biosynthetic genes, it remains to be clarified whether the verlamelin production is controlled by

transcriptional regulators.

Apart from the peptidyl moiety in the verlamelin structure, 5-hydroxytetradecanoic acid is the major component to be incorporated. However, no gene(s) encoding fatty acid synthase or polyketide synthase was present in the 50-kbp vicinity of *vlmS*, although fungal gene clusters for the fatty acid-containing compounds often possess a set of fatty acid synthase genes specific for the relevant component (Balakrishnam et al. 2013; Bhatnagar et al. 2003). Due to the fact that only a single set of genes encoding primary fatty acid synthase is present in the whole genome sequence of HF627, but no single PKS gene corresponding to tetradecanoic acid synthesis is present, the primary fatty acid synthase seems to synthesize the tetradecanoic acid, which should then be hydroxylated at position C5 by one of the *vlm* cluster enzymes to provide the immediate precursor, 5-hydroxytetradecanoic acid. The most likely candidate is VlmA (Fig. 4.4), which is highly similar (63% similarity) to ERG25 (NP_011574), which catalyzes hydroxylation of the C4-methyl group of 4,4-dimethylzymosterol (Bard et al. 1996). Indeed, feeding of 5-hydroxytetradecanoic acid to the *vlmA* disruptant could restore the production of verlamelin A in a dose-dependent manner to 7.7-23.4% of that in the wild-type, demonstrating that *vlmA* is involved in the synthesis of 5-hydroxytetradecanoic acid (Fig. 4.3). Similarly, feeding of 5-hydroxytetradecanoic acid to the *vlmB* disruptant could restore verlamelin production. VlmB shows similarity to acyl-CoA thioesterase in 4HBT family, and can be assumed to hydrolyze

fatty acyl-CoA, synthesized by fungal primary FAS (Tehlivets et al. 2007). However, when tetradecanoic acid was fed to *vlmB* disruptant, verlamelin production was not restored (data not shown), suggesting that *vlmB* is not functioning in the supply of tetradecanoic acid. Both the products of *vlmA* and *vlmB* are altogether regarded as essential components in the biosynthesis of 5-hydroxytetradecanoic acid, while the precise function of *vlmB* still remains to be solved.

To be loaded onto the waiting NRPS, 5-hydroxytetradecanoic acid should either be activated in the form of a CoA derivative by acyl-CoA ligase and transferred, in the manner of EasD (acyl-CoA ligase) and EasC (acyltransferase) in the emelliceramide biosynthesis (Chiang et al. 2008), or activated in the form of acyladenylate by an AMP-dependent ligase, in the manner of EcdI in echinocandin biosynthesis (Cacho et al. 2012). Because no acyltransferase-like genes are present, but only *vlmC*, which is homologous to AMP-dependent ligase gene, in the *vlm* cluster, verlamelin biosynthesis can be assumed to proceed via formation and loading of 5-hydroxytetradecanoyl adenylate onto VlmS.

Among the lipopeptide biosynthesis clarified in filamentous fungi, there are two pathways reported to supply the fatty acid moieties, as the cases of echicocandin B and apicidin, which contained C18 and C10 fatty acid moiety, respectively (Cacho et al. 2012; Jin et al. 2010). The in vitro experiment indicated that the C18 fatty acid moiety in echinocandin B comes from linoleic acid produced in primary metabolism, while the

decanoic acid used for the fatty amino acid moiety in apicidins was deduced to be synthesized by specific FAS complex, followed by oxidation and transamination to supply acyl amino acids as immediate substrate for the NRPS. Similar to the case of echinocandin B, tetradecanoyl moiety in verlamelins seems to be synthesized by the primary FAS, whereas further hydroxylation by VlmA is needed to provide immediate precursor to be incorporated. This study indicated a biosynthetic example of the fatty acid precursor for NRPS by partial modification of a fatty acid from primary metabolism, which has not been identified in fungal lipopeptide biosynthesis so far.

In this chapter, *vlm* biosynthetic gene cluster was isolated. Gene disruption and precursor feeding suggested that verlamelin biosynthesis may have the unique characteristic of a fatty acid moiety derived from primary metabolism.

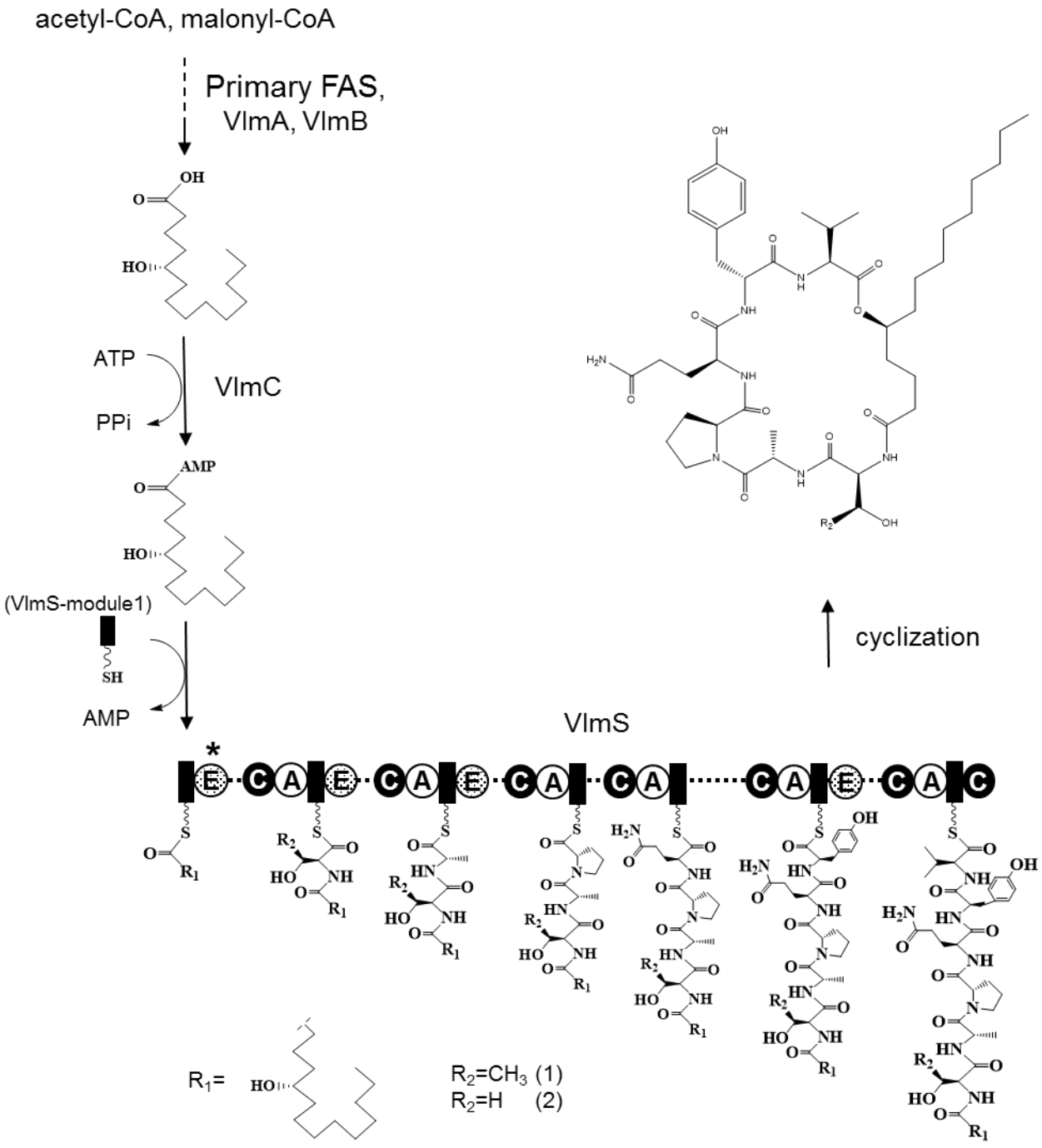

Fig. 4.4. Scheme of verlamelin biosynthesis proposed from this study. The white circles labeled A represent adenylation (A) domains. The black circles labeled C represent condensation (C) domains. The dotted circles labeled E represent epimerization (E) domains. The black boxes indicate peptidyl carrier protein (PCP) domains. *The E domain placed in the initial modules is considered to be inactive.

4.5 Summary

In this chapter, a gene cluster responsible for verlamelin biosynthesis was identified and characterized in order to study about the biosynthesis of verlamelin. A locus related to verlamelin biosynthesis was determined by disruption of NRPS genes transcribed in verlamelin producing conditions. In 50 kbp region of that NRPS suggested to be responsible for verlamelin biosynthesis by disruption, 10 ORFs other than NRPS gene was present. Only four genes, coding for NRPS (*vlmS*), fatty acid hydroxylase (*vlmA*), thioesterase (*vlmB*) and AMP-dependent ligase (*vlmC*), were found to be involved in the verlamelin biosynthesis in a 35-kbp region by the analysis of corresponding gene-knockouts. Surprisingly, no gene(s) coding for fatty acid synthase (FAS) or polyketide synthase (PKS) was present in the cluster, while verlamelin A/B contained a 5-hydroxytetradecanoic acid moiety. Precursor feeding experiment indicated that both *vlmA* and *vlmB* are involved in the biosynthesis of 5-hydroxytetradecanoic acid.

Biosynthesis of verlamelin was proposed based on the results described above. The primary FAS was likely responsible for the supply of tetradecanoil-CoA, putative precursor of 5-hydroxytetradecanoic acid moiety, which was then hydroxylated at C5 and thio-esterificated by VlmA and VlmB respectively, to provide 5-hydroxytetradecanoic acid. Putative AMP-dependent ligase, VlmC participated in the loading of the 5-hydroxytetradecanoic acid onto the initial PCP domain of VlmS. Peptide elongation and cyclization were accomplished by VlmS. The biosynthesis of

verlamelin was unique and characteristic compared to that of the other lipopeptide compounds especially in the part of fatty acid moiety.

Chapter 5

General conclusion

Genus *Lecanicillium* is a newly designated genus from the former *Verticillium lecanii,* and is belonging to entomopathogenic fungi used as an alternative of chemical pesticides in agricultural pest control. These classified into *Lecanicillium* are one of the most focused species because of their versatile activity against plant pathogenic fungi and nematode in addition to pest insects such as whiteflies and aphids. Judging from such abilities to kill or antagonize against a wide range of organisms, *Lecanicillium* has been assumed to produce various secondary metabolites.

Lipopeptides are compounds composed of fatty acid moieties and peptide moieties, including pharmaceutically important chemicals such as antifungal echinocandin or pneumocandin. Although the fatty acid moieties are important substructures to confer hydrophilic properties on the peptide moieties, the biosynthesis of the fatty acid moieties has not been well studied so far. Therefore, the biosynthesis of lipopeptides is required to be investigated, particularly with respect to the biosynthetic pathway of fatty acid moieties.

In this thesis, I clarified the biosynthetic pathway of cyclic lipodepsipeptides (verlamelin A and B) isolated from entomopathogenic fungus *Lecanicillium* sp. HF627. Furthermore, to make genetic study applicable for this strain, efficient and versatile transformation system was constructed.

In chapter 2, isolation and characterization of verlamelin and its new derivative are described. During my investigation about the secondary metabolites produced by *Lecanicillium* spp., verlamelin A (known lipopeptide compound) and its new derivative were isolated from the culture extract of *Lecanicillium* sp. HF627. Since the previous report did not mention the absolute configurations on the verlamelin structure, the structure of verlamelin was still ambiguous. Therefore, I determined the absolute structures of both verlamelin and its new derivative. As a result, the structures are determined unambiguously to be cyclo(5S-hydroxytetradecanoic acid-D-alloThr/Ser-D-Ala-L-Pro-L-Gln-D-Tyr-L-Val) for verlamelin A and B for the first time.

In chapter 3, I constructed transformation system of the verlamelin-producing strain *Lecanicillium* sp. HF627 in order to identify and analyze verlamelin biosynthetic genes. An easy transformation system was successfully developed by employing protoplast method using uridine auxotrophic mutant strain and *pyrG* gene which encodes orotidine 5-phosphate decarboxylase as the selection marker. In this system, both integrative and self-replicable vectors were constructed. To improve the low efficiency of homologous recombination, *ku80* gene which encodes a component of the non-homologous end joining machinery was deleted. Gene targeting efficiency for homologous recombination was enhanced, as exemplified by the efficiency increase to 62.5% using *trp1* and *his3* gene as the model in a *ku80* knockout host strain, while that was 19.6%

and 12.5%, respectively, in the original host strain. Thus, versatile transformation system for efficient genetic study in strain HF627 was constructed.

In chapter 4, I identified and characterized the biosynthetic gene cluster for verlamelin biosynthesis to obtain further knowledge of lipopeptide biosynthesis. Verlamelin biosynthetic gene cluster was proved to consist of four genes, *vlmS*, *vlmA*, *vlmB* and *vlmC*, encoding non-ribosomal peptide synthetase, fatty acid hydroxylase, acyl-CoA thioesterase and AMP-dependent ligase, respectively. Since neither the pathway-specific fatty acid synthase nor polyketide synthase gene was present around the cluster, 5-hydroxytetradecanoic acid (the component of the fatty acid moiety of verlamelin) was concluded to be supplied by primary fatty acid synthase. Feeding experiment suggested that both fatty acid hydroxylase and acyl-CoA thioesterase were involved to supply 5-hydroxytetradecanoic acid. It was considered that 5-hydroxytetradecanoic acid was transferred to the N-terminus of NRPS by AMP-dependent ligase via acyl-adenylate likewise the manner of the other lipopeptide biosynthesis. The following peptide elongation and cyclization was accomplished by NRPS.

Under this study, I isolated lipopeptide compounds, antifungal verlamelin A and B, produced by entomopathogenic fungus *Lecanicillium* sp. HF627 and determined the absolute structure for the first time. Furthermore, I proposed the biosynthetic pathway for verlamelins, based on the genetic analysis of verlamelin biosynthetic gene cluster.

Verlamelin biosynthetic gene cluster contains two unique genes, *vlmA* and *vlmB*, encoding fatty acid hydroxylase and acyl-CoA thioesterase, respectively. Since the participation of such gene(s) into the modification of fatty acid from primary metabolism has not been reported so far, this study should provide new insight into the lipopeptide biosynthesis in filamentous fungi.

Lipopeptide is regarded as a very important class of antibiotics in filamentous fungi, since it includes echinocandin-type lipopeptides which are developed and commercialized for treatment of fungal infection to immuno-compromised patients. Since the hydrophobicity or amphiphilicity is important for the activities of lipopeptide compounds, fatty acid moiety, the most hydrophilic part of lipopeptide compounds showld play crusial role for their biological activites. However, hydrophobicity of compounds may cause low water solvility, which hamper their effective use as drugs. To overcome this conflict, optimization of fatty acid substructure would be a solution since it may be possible to alter the hydrophobicity of these compounds balancing between bioactivities and water solubility. During the biosynthesis of verlamelin, the fatty acid precursor is assumed to be loaded onto VlmS via activation by AMP-dependent ligase which generally has relaxed substrate specificity. Judging from the successful complementation of the verlamelin production by external addition of fatty acid precursor, synthesis of new derivatives can be expected by feeding various fatty acids and/or manipulating the AMP-dependent ligase. Further analysis of the biosynthesis of

fatty acid moiety will contribute for creating new useful lipopeptide compounds.

Entomopathogenic fungi belonging to *Lecanicillium* have been used as versatile bio-pesticides all over world. However, the molecular basis of the pathogenicity have not been investigated due to the lack of suitable genetic tools. Although the host-vector system constructed in this study is specialized for strain HF627 so far, the result of this study demonstrated that genetic study is available in *Lecanicillium* using the same strategy for making transformation system or genetic tools as other filamentous fungi such as *Neurospora* or *Aspergillus*, where sophisticated molecular genetic studies have been conducted so far. Therefore, the construction of host-vector system in this study should be an important step for the efficient genetic study in *Lecanicillium* species.

Draft genome sequencing conducted in this study revealed that many biosynthetic genes for secondary metabolites were still to be identified on the genome of *Lecanicillium* sp. HF627. Although entomopathogenic fungi, including *Lecanicillium* sp. HF627, are considered to produce various bioactive compounds during infection to insects, only a limited number of compounds have been identified because most of biosynthetic genes may not expressed under laboratory conditions due to the rigid regulation on secondary metabolism. To utilize such unidentified compounds by inducing silent metabolic pathways, overexpression of the tightly regulated biosynthetic genes by promoter replacement or enhancement of the pathway specific activator will be the solutions, which can be achieved by genetic techniques such as *ku80* knockout

host strain or autonomously replicating vector developed in this thesis.

Detailed analysis of pathogenicity of entomopathogenic fungi in molecular level is important to improve their utility as bio-pesticide. Although a few reports have been available about relationship between secondary metabolism and pathogenicity of entomopathogenic fungi (Wang et al. 2012; Xu et al. 2008, 2009), the role of secondary metabolism in *Lecanicillium* spp. have not been investigated. Verlamelin, antifungal lipopeptide against plant pathogenic fungi including powdery mildew was found to be produced by *Lecanicillium* sp. Considering versatile activity of *Lecanicillium* against plant pathogenic fungi such as powdery mildew or rusts as well as pest insects (Goettel et al. 2008), it is highly likely that production of verlamelin participates in the antifungal activity of *Lecanicillium* spp. against plant pathogenic fungi. In this study, the biosynthetic genes for verlamelin were identified in *Lecanicillium* sp. HF627. Therefore, such knowledge about verlamelin biosynthesis in this study will be applicable to improve the utility of *Lecanicillium* spp., to create more useful bio-pesticide.

Reference

Amiri B, Ibrahim L, Butt TM (1999) Antifeedant properties of destruxins and their potential use with the entomogenous fungus *Metarhizium anisopliae* for improved control of crucifer pests. Biocont Sci Technol 9:487-498

Aranda FJ, Teruel JA, Ortiz A (2005) Further aspects on the hemolytic activity of the antibiotic lipopeptide iturin A. Biochim Biophys Acta 1713(1):51-56

Baba S, Abe Y, Ono C, Hosobuchi M (2006) Targeted disruption of the genes, *mlcR* and *ariB*, which encode GAL4-type proteins in *Penicillium citrinum*. Biochim Biophys Acta 1759(8):410-416

Balakrishnan B, Karki S, Chiu SH, Kim HJ, Suh JW, Nam B, Yoon YM, Chen CC, Kwon HJ (2013) Genetic localization and in vivo characterization of a *Monascus* azaphilone pigment biosynthetic gene cluster. Appl Microbiol Biotechnol 97:6337–6345

Baltz RH, Miao V, Wrigley SK (2005) Natural products to drugs: daptomycin and related lipopeptide antibiotics. Nat Prod Rep 22(6):717-741

Bandani AR, Khambay BPS, Faull JL, Newton R, Deadman M, Butt TM (2000) Production of efrapeptins by *Tolypocladium* species and evaluation of their insecticidal and antimicrobial properties. Mycol Res 104 (5):537-544

Bard M, Bruner DA, Pierson CA, Lees ND, Biermann B, Frye L, Koegel C, Barbuch R (1996) Cloning and characterization of ERG25, the *Saccharomyces cerevisiae* gene encoding C-4 sterol methyl oxidase. Proc Natl Acad Sci U S A 93(1):186-190

Benhamou N (2004) Potential of the mycoparasite, *Verticillium lecanii*, to protect citrus fruit against *Penicillium digitatum*, the causal agent of green mold: A comparison with

the effect of chitosan. Phytopathology 94(7):693-705

Bérdy J (2005) Bioactive microbial metabolites. J antibiot 58(1):1-26

Bérdy J (2012) Thoughts and facts about antibiotics: Where we are now and where we are heading. J antibiot 65(8):385-395

Bhatnagar D, Ehrlich KC, Cleveland TE (2003) Molecular genetic analysis and regulation of aflatoxin biosynthesis. Appl Microbiol Biotechnol 61(2):83-93

Bhushan R, Bruckner H (2004) Marfey's regent for chiral amino acid analysis: A review. Amino acids 27:231-247

Bird D, Bradshaw R (1997) Gene targeting is locus dependent in the filamentous fungus *Aspergillus nidulans*. Mol Gen Genet 255(2):219-225

Brakhage AA, Schroeckh V (2011) Fungal secondary metabolites–strategies to activate silent gene clusters. Fungal Genet Biol 48(1):15-22

Brückner B, Unkles SE, Weltring K, Kinghorn JR (1992) Transformation of *Gibberella fujikuroi*: effect of the *Aspergillus nidulans* AMA1 sequence on frequency and integration. Curr Genet 22(4):313-316

Cacho RA, Jiang W, Chooi YH, Walsh CT, Tang Y (2012) Identification and characterization of the echinocandin B biosynthetic gene cluster from *Emericella rugulosa* NRRL 11440. J Ame Chem Soci 134(40):16781-16790

Chang PK, Scharfenstein LL, Wei Q, Bhatnagar D (2010) Development and refinement of a high-efficiency gene-targeting system for *Aspergillus flavus*. J microbiol methods 81(3):240-246

Chiang YM, Szewczyk E, Nayak T, Davidson AD, Sanchez JF, Lo HC, Ho WY, Simityan H, Kuo E, Praseuth A, Watanabe K, Oakley BR, Wang CC (2008) Molecular Genetic Mining of the *Aspergillus* Secondary Metabolome: Discovery of the Emericellamide Biosynthetic Pathway. Chem Biol 15(6):527-532

Claydon N, Grove JF, Pople M, Begley MJ (1984) New metabolic products of *Verticillium lecanii*. Part 1. 3β-Hydroxy-4, 4, 14α-trimethyl-5α-pregna-7, 9 (11)-diene-20S-carboxylic acid and the isolation and characterisation of some minor metabolites. J Chem Soc Perkin Trans 1:497-502

da Silva Ferreira ME, Kress MR, Savoldi M, Goldman MHS, Härtl A, Heinekamp T, Brakhage AA, Goldman GH (2006) The *akuB*^{KU80} mutant deficient for nonhomologous end joining is a powerful tool for analyzing pathogenicity in *Aspergillus fumigatus*. Eukaryotic cell 5(1):207-211

Deleu M, Paquot M, Nylander T (2005) Fengycin interaction with lipid monolayers at the air-aqueous interface-implications for the effect of fengycin on biological membranes. J Coll Int Sci 283(2):358-365

Dewick PM (2009) Medicinal Natural Products: A Biosynthetic Approach 3rd edition. Wiley, Hoboken, NJ

Douglas CM, Foor F, Marrinan JA, Morin N, Nielsen JB, Dahl AM, Mazur P, Baginsky W, Li W, El-Sherbeini M, Clemas JA, Mandala SM, Frommer BR, Kurtz MB (1994) The *Saccharomyces cerevisiae FKS1* (*ETG1*) gene encodes an integral membrane protein which is a subunit of 1, 3-beta-D-glucan synthase. Proc Nat Acad Sci U S A 91(26):12907-12911

Fang W, Zhang Y, Yang X, Zheng X, Duan H, Li Y, Pei Y. (2004) *Agrobacterium*

tumefaciens-mediated transformation of *Beauveria bassiana* using an herbicide resistance gene as a selection marker. J Invertebr Pathol 85(1): 18-24

Faria MR, Wraight SP (2007) Mycoinsecticides and Mycoacaricides: A comprehensive list with worldwide coverage and international classification of formulation types. Biolog Cont 43:237–256

Fierro F, Kosalková K, Gutiérrez S, Martín JF (1996) Autonomously replicating plasmids carrying the AMA1 region in *Penicillium chrysogenum*. Curr Genet 29(5):482-489

Fleming A (1929) On the antibacterial action of cultures of a *penicillium*, with special reference to their use in the isolation of *B. influenzae*. Br J Exp Pathol 10(3):226-236

Fujie A, Iwamoto T, Muramatsu H, Okudaira T, Nitta K, Nakanishi T, Sakamoto K, Hori Y, Hino M, Hashimoto S, Okuhara M (2000) FR901469, a novel antifungal antibiotic from an unidentified fungus No. 11243. I. Taxonomy, fermentation, isolation, physico-chemical properties and biological properties. J Antibiot 53(9):912-919

Gao X, Haynes SW, Ames BD, Wang P, Vien LP, Walsh CT, Tang Y (2012) Cyclization of fungal nonribosomal peptides by a terminal condensation-like domain. Nat Chem Biol 8(10):823-830

Gelb MH, Jain MK, Berg OG (1994) Inhibition of phospholipase A2. FASEB J 8(12):916-924.

Gems D, Johnstone IL, Clutterbuck AJ (1991) An autonomously replicating plasmid transforms *Aspergillus nidulans* at high frequency. Gene 98(1):61-67

Goettel MS, Koike M, Kim JJ, Aiuchi D, Shinya R, Brodeur J (2008) Potential of

Lecanicillium spp. for management of insects, nematodes and plant diseases. J Invertebr Pathol 98(3):256-261

Grove JF (1984) 23, 24, 25, 26, 27-Pentanorlanost-8-en-3β, 22-diol from *Verticillium lecanii*. Phytochemistry 23(8):1721-1723

Guangtao Z, Hartl L, Schuster A, Polak S, Schmoll M, Wang T, Seidl V, Seiboth B (2009) Gene targeting in a nonhomologous end joining deficient *Hypocrea jecorina*. J Biotechnol 139(2):146-151

Gulick AM (2009) Conformational dynamics in the Acyl-CoA synthetases, adenylation domains of non-ribosomal peptide synthetases, and firefly luciferase. ACS Chem Biol 4(10):811-827

Haritakun R, Sappan M, Suvannakad R, Tasanathai K, Isaka M (2009) An antimycobacterial cyclodepsipeptide from the entomopathogenic fungus *Ophiocordyceps communis* BCC 16475. J Nat Prod 73(1):75-78

Hasan S, Singh RI, Singh SS (2011) Development of Transformation System of *Verticillium lecanii* (*Lecanicillium* spp.) (Deuteromycotina: Hyphomycetes) Based on Nitrate Reductase Gene of Aspergillus nidulans. Ind J Microbiol 51(3):390-395

Haynes SW, Ames BD, Gao X, Tang Y, Walsh CT (2011) Unraveling terminal C-domain-mediated condensation in fungal biosynthesis of imidazoindolone metabolites. Biochemistry 50(25):5668-5679

Hsu HL, Yannone SM, Chen DJ (2001) Defining interactions between DNA-PK and ligase IV/XRCC4. DNA Repair 1:225-235

Isaka M, Kittakoop P, Kirtikara K, Hywel-Jones NL, Thebtaranonth Y. (2005) Bioactive

substances from insect pathogenic fungi. Acc Chem Res 38(10):813-823

Ishibashi K, Suzuki K, Ando Y, Takakura C, Inoue H (2006) Nonhomologous chromosomal integration of foreign DNA is completely dependent on MUS-53 (human Lig4 homolog) in *Neurospora*. Proc Natl Acad Sci 103(40):14871-14876

Jin JM, Lee S, Lee J, Baek SR, Kim JC, Yun SH, Park SY, Kang S, Lee YW (2010) Functional characterization and manipulation of the apicidin biosynthetic pathway in *Fusarium semitectum*. Mol Microbiol 76(2):456-466

Jirakkakul J, Punya J, Pongpattanakitshote S, Paungmoung P, Vorapreeda N, Tachaleat A, Klomnara C, Tanticharoen M, Cheevadhanarak S (2008) Identification of the nonribosomal peptide synthetase gene responsible for bassianolide synthesis in wood-decaying fungus *Xylaria* sp. BCC1067. Microbiology 154(4):995-1006

Kasai Y, Taji H, Fujita T, Yamamoto Y, Akagi M, Sugio A, Kuwahara S, Watanabe M, Harada N, Ichikawa A, Schurig V (2004) MαNP acid, a powerful chiral molecular tool for preparation of enantiopure alcohols by resolution and determination of their absolute configurations by the ^{1}H NMR anisotropy method. Chirality, 16(9):569-585

Keller NP, Turner G, Bennett JW (2005) Fungal secondary metabolism—from biochemistry to genomics. Nat Rev Microbiol 3(12):937-947

Kim JC, Choi GJ, Kim HJ, Kim HT, Ahn JW, Cho KY (2002) Verlamelin, an antifungal compound produced by a mycoparasite, *Acremonium strictum*. Plant Pathol J 18(2):102-105

Kim JJ, Goettel MS, Gillespie DR (2007) Potential of *Lecanicillium* species for dual microbial control of aphids and the cucumber powdery mildew fungus, *Sphaerotheca fuliginea*. Biological Control 40(3):327-332

Kusumi T, Yabuuchi T, Takahashi H, Ooi T (2005) Chiral anisotropic reagents for determining the absolute configulation of secondary alcohols and carboxylic acids. Yuki gosei kagaku kyokaishi 63(11):1102-1114.

Li M, Zhou L, Liu M, Huang Y, Sun X, Lu F (2013) Construction of an Engineering Strain Producing High Yields of α-Transglucosidase via *Agrobacterium tumefaciens*-Mediated Transformation of *Asperillus niger*. Biosci Biotechnol Biochem 77(9):1860-1866

Mandal SM, Barbosa AE, Franco OL (2013) Lipopeptides in microbial infection control: scope and reality for industry. Biotechnol Adv 31(2):338-345

Marahiel MA, Stachelhaus T, Mootz HD (1997) Modular peptide synthetases involved in nonribosomal peptide synthesis. Chem Rev 97(7):2651-2674

Meek K, Gupta S, Ramsden DA, Lees Miller SP (2004) The DNA‐dependent protein kinase: the director at the end. Immunol Rev 200(1):132-141

Meyer SL, Meyer RJ (1996) Greenhouse studies comparing strains of the fungus *Verticillium lecanii* for activity against the nematode *Heterodera glycines*. Fund Appl Nematol 19(3):305-308

Molnár I, Gibson DM, Krasnoff SB (2010) Secondary metabolites from entomopathogenic Hypocrealean fungi. Nat Prod Rep 27(9):1241-1275

Muraih JK, Pearson A, Silverman J, Palmer M (2011) Oligomerization of daptomycin on membranes. Biochim Biophys Acta 1808(4):1154-1160

Nagashima K, Ikeda T, Yasokawa D, Nakagawa R (1994) Isolation of auxotrophic mutants of *Monascws* species (beni koji fungi). Bull Hokkaido Food Process Res Center

1:57-60

Nakazawa T, Ando Y, Kitaaki K, Nakahori K, Kamada T (2011) Efficient gene targeting in *ΔCc.ku70* or *ΔCc.lig4* mutants of the agaricomycete *Coprinopsis cinerea.* Fungal Genet Biol 48:939–946

Nayak T, Szewczyk E, Oakley CE, Osmani A, Ukil L, Murray SL, Hynes MJ, Osmani SA, Oakley BR (2006) A versatile and efficient gene-targeting system for *Aspergillus nidulans*. Genetics 172(3):1557-1566

Nguyen NV, Kim YJ, Oh KT, Jung WJ, Park RD (2007) The role of chitinase from *Lecanicillium antillanum* B-3 in parasitism to root-knot nematode *Meloidogyne incognita* eggs. Biocontrol Sci Tech 17(10):1047-1058

Nihei K, Itoh H, Hashimoto K, Miyairi K, Okuno T (1998) Antifungal cyclodepsipeptides, W493 A and B, from *Fusarium* sp.: isolation and structural determination. Biosci Biotechnol Biochem 62(5):858-863

Ninomiya Y, Suzuki K, Ishii C, Inoue H (2004) Highly efficient gene replacements in *Neurospora* strains deficient for nonhomologous end-joining. Proc Natl Acad Sci 101(33):12248-12253

Onishi J.C., Rowin G.L. Miller J.E. (1980). Antibiotic A43F. United States Patent 4201771. May 6, 1980.

Ostroumova OS, Malev VV, Ilin MG, Schagina LV (2010) Surfactin activity depends on the membrane dipole potential. Langmuir 26(19):15092-15097

Pastink A, Eeken JC, Lohman PH (2001) Genomic integrity and the repair of double-strand DNA breaks. Mutat Res 480:37-50

Pöggeler S, Kück U (2006) Highly efficient generation of signal transduction knockout mutants using a fungal strain deficient in the mammalian *ku70* ortholog. Gene 378:1–10

Roll DM, Barbieri LR, Bigelis R, McDonald LA, Arias DA, Chang LP, Singh MP, Luckman SW, Berrodin TJ, Yudt MR (2009) The Lecanindoles, Nonsteroidal Progestins from the Terrestrial Fungus *Verticillium lecanii* 6144. J Nat Prod 72(11):1944-1948

Rowin GL, Miller JE, Albers-Schönberg G, Onishi JC, Davis D, Dulaney EL (1986) Verlamelin, a new antifungal agent. J Antibiot 39(12):1772-1775

Shimizu T (2006$_a$) Cloning and functional analysis of genes involved in biosynthesis of mycotoxin citrinin from *Monascus purpureus*. Dissertation, Osaka University

Shimizu T, Kinoshita H, Nihira T (2006$_b$) Development of transformation system in *Monascus purpureus* using an autonomous replication vector with aureobasidin A resistance gene. Biotechnol Lett. 28(2):115-120

Shimizu T, Kinoshita H, Nihira T (2007) Identification and in vivo functional analysis by gene disruption of *ctnA*, an activator gene involved in citrinin biosynthesis in *Monascus purpureus*. Appl Environ Microbiol 73(16):5097-5103

Shimizu T, Ito T, Kanematsu S (2012) Transient and multivariate system for transformation of a fungal plant pathogen, *Rosellinia necatrix*, using autonomously replicating vectors. Curr Genet 58:129–138

Singkaravanit S (2010$_a$) Isolation and functional analysis of GGPP synthase gene involved in isoprenoid biosynthesis from entomopathogenic fungi. Dissertation, Osaka University

Singkaravanit S, Kinoshita H, Ihara F, Nihira T (2010$_b$) Cloning and functional analysis

of the second geranylgeranyl diphosphate synthase gene influencing helvolic acid biosynthesis in *Metarhizium anisopliae*. Appl Microbiol Biotechnol 87(3):1077-1088

Slightom JL, Metzger BP, Luu HT, Elhammer AP (2009) Cloning and molecular characterization of the gene encoding the Aureobasidin A biosynthesis complex in *Aureobasidium pullulans* BP-1938 Gene 431(1):67-79

Soman AG, Gloer JB, Angawi RF, Wicklow DT, Dowd PF (2001) Vertilecanins: New Phenopicolinic Acid Analogues from *Verticillium lecanii*. J Nat Prod 64(2):189-192

Staats CC, Junges A, Fitarelli M, Furlaneto MC, Vainstein MH, Schrank A (2007). Gene inactivation mediated by *Agrobacterium tumefaciens* in the filamentous fungi *Metarhizium anisopliae*. Appl Microbiol Biotechnol 76(4):945-950

Strasser H, Abendstein D, Stuppner H, Butt TM (2000) Monitoring the distribution of secondary metabolites produced by the entomogenous fungus *Beauveria brongniartii* with particular reference to oosporein. Mycol Res 104 (10):1227-1233

Takahashi T, Masuda T, Koyama Y (2006) Enhanced gene targeting frequency in *ku70* and *ku80* disruption mutants of *Aspergillus sojae* and *Aspergillus oryzae*. Mol Genet Genomics 275(5):460-470

Takita Y, Takahara M, Nogami S, Anraku Y, Ohya Y (1997) Applications of the long and accurate polymerase chain reaction method in yeast molecular biology: direct sequencing of the amplified DNA and its introduction into yeast. Yeast 13(8):763-768

Tehlivets O, Scheuringer K, Kohlwein SD (2007) Fatty acid synthesis and elongation in yeast. Biochim Biophys Acta 1771(3):255-270

Villalba F, Collemare J, Landraud P, Lambou K, Brozek V, Cirer B, Morin D, Bruel C,

Beffa R, Lebrun MH (2008) Improved gene targeting in *Magnaporthe grisea* by inactivation of *MgKU80* required for non-homologous end joining. Fungal Genet Biol 45(1):68-75

Wang B, Kang Q, Lu Y, Bai L, Wang C (2012) Unveiling the biosynthetic puzzle of destruxins in *Metarhizium* species. Proc Nat Acad Sci U S A 109(4):1287-1292

Wiederhold NP, Lewis RE (2003) The echinocandin antifungals: an overview of the pharmacology, spectrum and clinical efficacy. Exp Opin Inv Drug 12(8):1313-1333

Wiest A, Grzegorski D, Xu BW, Goulard C, Rebuffat S, Ebbole DJ, Bodo B, Kenerley C (2002) Identification of peptaibols from *Trichoderma virens* and cloning of a peptaibol synthetase. J Biol Chem 277(23):20862-20868

Xu Y, Orozco R, Kithsiri Wijeratne EM, Espinosa-Artiles P, Leslie Gunatilaka AA, Patricia Stock S, Molnár I (2009) Biosynthesis of the cyclooligomer depsipeptide bassianolide, an insecticidal virulence factor of *Beauveria bassiana*. Fungal Genet Biol 46(5):353-364

Xu Y, Orozco R, Wijeratne EM, Gunatilaka AA, Stock SP, Molnár I (2008) Biosynthesis of the cyclooligomer depsipeptide beauvericin, a virulence factor of the entomopathogenic fungus *Beauveria bassiana*. Chem Biol 15(9):898-907

Yu JH, Butchko RA, Fernandes M, Keller NP, Leonard TJ, Adams TH (1996) Conservation of structure and function of the aflatoxin regulatory gene *aflR* from *Aspergillus nidulans* and *A. flavus*. Curr genet 29(6):549-555

Yu X, Gabriel A (2003) Ku-dependent and Ku-independent end-joining pathways lead to chromosomal rearrangements during double-strand break repair in *Saccharomyces cerevisiae*. Genetics 163(3):843-856

Related publications

1. **Ishidoh K**, Kinoshita H, Ihara F, Nihira T (2014) Efficient and versatile transformation systems in entomopathogenic fungus *Lecanicillium* species. Curr Genet 60(2):99-108

2. **Ishidoh K**, Kinoshita H, Igarashi Y, Ihara F, Nihira T (2014) Cyclic lipodepsipeptides verlamelin A and B, isolated from entomopathogenic fungus *Lecanicillium* sp.. J Antibiot 67:459-463

3. **Ishidoh K**, Kinoshita H, Nihira T (2014) Identification of a gene cluster responsible for the biosynthesis of cyclic lipopeptide verlamelin. Appl Microbiol Biotechnol 98:7501-7510

Acknowledgement

I would like to express my deepest gratitude to my supervisor, Professor Takuya Nihira of ICBiotech, for his guidance and valuable advice. I am also grateful to our Assistant Professor Hiroshi Kinoshita, for his support, comments and suggestions throughout the conduct of this study. I also would like to express my sincere thanks to Associate Professor Shigeru Kitani for his support and kindness.

My sincere thanks are due to Professor Satoshi Harashima and Professor Toshiya Muranaka for their detailed review and excellent advice in the preparation of this thesis.

I wish to extend my warm thanks to the member of our laboratory (Nihira lab.) and ICBiotech members.